The manuscript by Fischer et al., presents tropospheric measurements of satellite retrieved peroxyacetyl nitrate (PAN) over North America and investigates the changes in concentrations linked to fires. Overall, the manuscript would be a nice addition to the existing literature (e.g. Payne et al., 2014, 2016) as there are limited flight campaigns measuring PAN and MIPAS can only retrieve it in the UTLS. The compositing of TES PAN retrievals under smoke plumes is also an interesting way to investigate potential enhancements of PAN related to fires. Therefore, once the comments below are addressed, this manuscript should be accepted for publication in ACP.

Major comments:

As TES is the only satellite currently measuring lower tropospheric PAN (to the best of my knowledge anyway), it would be useful to see the spatial distribution of PAN at different tropospheric levels. In neither this paper nor the Payne et al., (2014, 2016) manuscripts, there are very few spatial maps of TES PAN. In Payne et al., (2016), Figure 1a shows a noisy spatial distribution of TES PAN in the tropics. Therefore, it would be useful if this study could add another figure (e.g. between Figure 1 and Figure 2) showing the PAN distribution over N. America (e.g. the July 2006-2009 average on a regular grid instead of individual retrievals on several tropospheric levels) highlighting the average PAN hotspots and potential outflow of PAN from source regions.

We agree that showing a spatial distribution is interesting. Exactly as suggested, we have added the July 2006-2009 average on a regular 2x2 degree grid. However, we have only done this as a tropospheric average. As discussed in Payne et al. (2014) and also in Section 2.1, the TES PAN retrievals do not provide information on the vertical variation of PAN. In all cases, the degrees of freedom for signal, or number of independent pieces of vertical information in the retrieval, is less than 1.0. To address the true spirit of this suggestion we have also added a panel that shows all the data points individually; this allows readers to see the noise in the data. We also include the entire region of retrievals that were processed so that readers can view the distribution off-land as well. We have added another paragraph describing this new Figure (now Figure 2 as suggested) in section 2.1.

"Figure 2 shows the July 2006 – 2009 tropospheric average PAN. When all the existing TES data is gridded, there are several large patterns that emerge. 1) Average tropospheric PAN mixing ratios in the TES observations generally increase with latitude during the month of July over North America. 2) Average tropospheric PAN mixing ratios generally decrease from west to east. 3) As can be seen in later figures, there are relatively few retrievals per grid box over the southwestern U.S. Though there are relatively few samples (~5-20 per 2x2°grid box), relatively high mixing ratios (0.6 ppbv) are observed over the Colorado Front Range.

The presentation of the manuscript needs to be improved as several of the Figures have been mislabelled in the text and it is difficult to follow. In Figure 7, there is reference to red lines, but all the lines are grey/black, again making it difficult to read the paper.

We apologize for the labels on the original Figure 7. We changed the lines from red to black and color-coordinated the dots with the original Figure 6, and then it looks like only half of the caption for the original Figure 7 was updated. We have fixed this.

Section 3.3 needs to be made clearer as discussion of the PAN:CO ratios is rather rushed. For instance, adding some equations into Section 3.3 on how the enhancement ratios are calculated would be useful. Again, as Figure 7 has misleading colours, it is difficult to work out what the authors are trying to say in this section.

We sincerely believe that this section is now much easier to understand with the caption for Figure 7 (now Figure 8) corrected. As indicated in the comment above and noted by the second reviewer, we mislabeled black lines as red in the submitted caption. There was also an incorrect reference to Figure 7 (now Figure 8) in Section 3.3, which should have pointed readers to Figure 6 (now Figure 7). Now that these typos

have been fixed, this section should be much easier to follow. However, as suggested by the reviewer, we have also added an equation describing the calculation of the PAN enhancement ratios, and several sentences at the start of the section that point readers to a reference that discusses enhancement ratios and their pitfalls (Yokelson et al., 2013). There are two key points to this section, and we now state both of them in the introductory paragraph. 1) The tropospheric PAN enhancement ratios from TES fall within the range of relevant aircraft measurements over North America. 2) There are many pitfalls associated with using enhancement ratios as observed from TES to study the evolution of PAN in the smoke plumes we have identified here.

Minor comments:
P1 L68: Would be good to reference of Ungermann et al., (2016) who investigate PAN in the summer-time Asian monsoon region using Earth observation measurements. On Line 62-64, the authors states "much of our understanding of the distribution of PAN outside urban areas rests on data from aircraft missions interpreted with global chemical transport models". I think it would be useful to reference a few papers that have utilised CTMs and satellite data to investigate PAN (e.g. Fadnavis et al., 2014; Pope et al., 2016).

Thank you very much for pointing out these newer references. We have added citations to all of them in the suggested locations.

P2 L102: What do the authors mean by "True profiles"? In Figure 1, would the true profile by the retrieved profile?

The "true profile" is the actual atmospheric profile. We have updated the caption and text to indicate this.

P2 L106-107: "As discussed in Payne et al. (2014), the TES PAN retrievals do not provide information on the vertical variation of PAN". This does not make sense. PAN is retrieved at several vertical levels and the AKs will provide information on the vertical sensitivity. P2 L107-109: IF a DOF < 1 means a retrieval is heavily influenced by the aprioi then why do the authors often use the criteria of the DOF > 0.6?

This threshold value of DOF > 0.6 was chosen to be consistent with a signal to noise ratio (SNR) greater than 1 (Payne et al. 2014), and this criteria has been used in all the papers that have presented TES PAN data thus far. We have added these sentences to the manuscript to clarify this choice. It is also worth noting that the shape of the retrieved profile is always heavily influenced by the shape of the a priori profile for these measurements (see response to next comment).

P3 L128-129: The authors state TES has sensitivity to enhanced PBL PAN, but the concentrations are much lower than that of the aircraft?

For nadir retrievals of molecules with weak spectral signatures where the DOFS <1.0, the shape of the retrieved profile is heavily influenced by the shape of the prior. Since the prior profile for this case peaks in the mid-troposphere, the retrieved profile will also peak in the mid-tropopshere. A large enhancement in boundary layer PAN shows up in the TES radiances as a small enhancement in the PAN signal. A small enhancement in the mid-troposphere would also show up in the TES radiances as a small enhancement in the PAN signal. The nature of the measurement is such that it is not possible to distinguish between these two scenarios in the TES radiances. An example is provided in Figure 2 in Payne et al. (2014). Therefore, although we demonstrate for this case that TES has some sensitivity to elevated PAN in the boundary layer, for the more general case where we do not have co-located in-situ profile measurements, we would only be able to say that there is some enhancement in PAN somewhere in the column.

We have added this discussion to the second to last paragraph of section 2.1. This now reads:

"The peak sensitivity for PAN is generally between 400 – 800 hPa (Payne et al., 2014), but a comparison between TES PAN transect observations coincident with Front Range Air Pollution and Photochemistry Éxperiment (FRAPPÉ) observations (Figure 2) show that TES can have some degree of sensitivity to PAN in the boundary layer when boundary layer PAN is elevated. As an example, Figure 3 presents in situ observations from a flight during FRAPPÉ made with a thermal dissociation chemical ionization mass

spectrometer (TD-CIMS) (Zheng et al., 2011). Mean PAN observed by the C-130 below 3 km during the field campaign was 481 pptv (Zaragoza et al., 2017). This particular day (29 July) was one of the four days identified by Zaragoza et al. (2017) with the highest surface PAN mixing ratios observed at the Boulder Atmospheric Observatory. The overlaid TES data in Figure 3a (parallelograms) show an enhancement in the TES PAN (as shown by the TES observation highlighted by a black square) in the vicinity of aircraft measurements of highly elevated PAN values in the boundary layer indicating that in this case TES is weakly sensitive to the elevated boundary layer values despite the presence of high clouds (dashed line Figure 3c). Figure 3 also shows red and blue lines corresponding to application of the averaging kernel for this case to hypothetical "true" profiles with and without the enhancement in the boundary layer. The red and blue lines show that TES has some sensitivity to PAN below 800 hPa, but the retrieval places the additional PAN higher up in the atmosphere. While the difference between the red and the blue solid lines in Figure 3d is small, it is non-zero indicating that TES has some sensitivity to the boundary layer enhancement in this case."

P3 L127-128: Add tropospheric column definition to the Figure 2 caption.

This information was added. Figure 2 is now Figure 3.

P4 L 153-154: Please explain "i.e. matching based only on UTC day" more clearly.

Matching by UTC day is explained in the following sentences, but we added on additional one for clarification. This now reads: "We matched all TES PAN retrievals based on UTC day. This means that overnight retrievals are paired with the plume from the prior day. As discussed in Brey et al. (2017), most of the large wildfire plumes occurring in July over the western U.S. are very large and last several days. So we would expect that pairing the overnight retrievals with the plume from the prior day (i.e. matching based only on UTC day) is not likely to change our results, and that to be the case. We have repeated all our calculations using only the daytime retrievals, and the choice to use all the retrievals does not change the results."

P4 L178: Do the authors mean Supplementary Figure (SF) 2 not SF1? Also, why is the red axis (number of attempts) over the Pacific Ocean? This needs to be explained more clearly?

Yes, we mean Supplementary Figure 2. This typo has been corrected. The second comment is also the product of a typo in the caption for Supplementary Figure 2. This sentence is supposed to point readers to a comparable figure in Zhu et al. (2017), but that reference is missing. Similar data for the Pacific Ocean is presented there for the same set of months. This has been fixed.

P4 L180: Figure 3c instead of 3a?

Yes, this should refer to 3c instead of 3a. This has been corrected.

P7 L 259: Coloured dots? I can only see purple dots.

Yes, this should say purple to be less confusing. This has been fixed by adding a more specific sentence.

"Figure 8 presents a histogram of PAN enhancement ratios in the subset of retrievals that overlap HMS smoke polygons and also are likely to have elevated PAN and CO in the free troposphere (TES CO > 150 hPa). The purple dots designate the two retrievals shown in Figure 7 that meet these strict criteria."

Figure 2b: Why is there such a large discrepancy between aircraft (blue) and TES (black) PAN?

As discussed above, for nadir retrievals of molecules with weak spectral signatures where the DOFS <1.0, the shape of the retrieved profile is heavily influenced by the shape of the prior. Since the prior profile for this case peaks in the mid-troposphere, the retrieved profile will also peak in the mid-tropopshere. A large enhancement in boundary layer PAN shows up in the TES radiances as a small enhancement in the PAN

signal. A small enhancement in the mid-troposphere would also show up in the TES radiances as a small enhancement in the PAN signal. The nature of the measurement is such that it is not possible to distinguish between these two scenarios in the TES radiances. An example is provided in Figure 2 in Payne et al. [2014]. Therefore, although we demonstrate for this case that TES has some sensitivity to elevated PAN in the boundary layer, for the more general case where we do not have co-located in-situ profile measurements, we would only be able to say that there is some enhancement in PAN somewhere in the column.

As discussed above, we have added more text to this section. We are not claiming good sensitivity to the boundary layer. This example provides the first direct evidence of any sensitivity to PAN in the boundary layer for TES.

Figure 2d: Worth adding equation in main text or caption how the AKs are applied.

We have added substantial additional text and equations to Section 2.1 to address this comment.

Figure 2d: The difference between the red and blue solid lines looks tiny, so how does this show TES has good sensitivity?

We have not tried to claim "good" sensitivity. Rather this example shows that TES has some sensitivity. To make this clear, we have again added substantially more details to the latter part of Section 2.1, in particular, the updated paragraph now reads:

"The peak sensitivity for PAN is generally between 400 – 800 hPa (Payne et al., 2014), but a comparison between TES PAN transect observations coincident with Front Range Air Pollution and Photochemistry Éxperiment (FRAPPÉ) observations (Figure 2) show that TES can have some degree of sensitivity to PAN in the boundary layer when boundary layer PAN is elevated. As an example, Figure 3 presents in situ observations from a flight during FRAPPÉ made with a thermal dissociation chemical ionization mass spectrometer (TD-CIMS) (Zheng et al., 2011). Mean PAN observed by the C-130 below 3 km during the field campaign was 481 pptv (Zaragoza et al., 2017). This particular day (29 July) was one of the four days identified by Zaragoza et al. (2017) with the highest surface PAN mixing ratios observed at the Boulder Atmospheric Observatory. The overlaid TES data in Figure 3a (parallelograms) show an enhancement in the TES PAN (as shown by the TES observation highlighted by a black square) in the vicinity of aircraft measurements of highly elevated PAN values in the boundary layer indicating that in this case TES is weakly sensitive to the elevated boundary layer values despite the presence of high clouds (dashed line Figure 3c). Figure 3 also shows red and blue lines corresponding to application of the averaging kernel for this case to hypothetical "true" profiles with and without the enhancement in the boundary layer. The red and blue lines show that TES has some sensitivity to PAN below 800 hPa, but the retrieval places the additional PAN higher up in the atmosphere. While the difference between the red and the blue solid lines in Figure 3d is small, it is non-zero indicating that TES has some sensitivity to the boundary layer enhancement in this case."

Figure 6: Useful to add a CALIPSO track line to the top panel map. . .i.e. where did CALIPSO cross the domain?

This was included in the figure already as a dashed line labeled "CALIPSO Overpass".

Figure 7: Where are the red lines/dots?

We apologize for the labels on the original Figure 7. We changed the lines from red to black and color-coordinated the dots with the original Figure 6, and then it looks like only half of the caption for the original Figure 7 was updated. We have fixed this.

Figure 8: State that the data is from ARCTAS.

As suggested, we have changed the first sentence of the caption to also directly reference ARCTAS and not just Hecobian et al. (2011). This reads "Histogram of estimated PAN enhancement ratios based on in situ measurements of fire plumes described in Hecobian et al. (2011) from the ARCTAS campaign."

Figure S2: How do the authors define "elevated PAN"?

We have removed this wording because it is confusing. TES has a high detection limit, and that is already stated in the methods. This word was not needed here.

References:

Fadnavis, S., Schultz, M. G., Semeniuk, K., Mahajan, A. S., Pozzoli, L., Sonbawne, S., Ghude, S. D., Kiefer, M., and Eckert, E.: Trends in peroxyacetyl nitrate (PAN) in the upper troposphere and lower stratosphere over southern Asia during the summer monsoon season: regional impacts, Atmos. Chem. Phys., 14, 12725–12743, doi:10.5194/acp-14-12725-2014, 2014.

Payne, V. H., Alvarado, M. J., Cady-Pereira, K. E., Worden, J. R., Kulawik, S. S., and Fischer, E. V.: Satellite observations of peroxyacetyl nitrate from the Aura Tropospheric Emission Spectrometer, Atmos. Meas. Tech., 7, 3737-3749, 10.5194/amt-7-3737- 2014, 2014.

Payne, V. H., Fischer, E. V., Worden, J. R., Jiang, Z., Zhu, L., Kurosu, T. P., and Kulawik, S. S.: Spatial variability in tropospheric peroxyacetyl nitrate in the tropics from infrared satellite observations in 2005 and 2006, Atmos. Chem. Phys. Discuss., 2016, 121, 10.5194/acp-2016-1047, 2016.

Pope, R. J., Richards, N. A. D., Chipperfield, M. P., Moore, D. P., Monks, S. A., Arnold, S. R., Glatthor, N., Kiefer, M., Breider, T. J., Harrison, J. J., Remedios, J. J., Warneke, C., Roberts, J. M., Diskin, G. S., Huey, L. G., Wisthaler, A., Apel, E. C., Bernath, P. F., and Feng, W.: Intercomparison and evaluation of satellite peroxyacetyl nitrate observations in the up- per troposphere–lower stratosphere, Atmos. Chem. Phys., 16, 13541–13559, doi:10.5194/acp-16-13541-2016, 2016.

Ungermann, J., Ern, M., Kaufmann, M., Müller, R., Spang, R., Ploeger, F., Vogel, B., and Riese, M.: Observations of PAN and its confinement in the Asian summer monsoon anticyclone in high spatial resolu

All suggested references have been added.

In this manuscript, the authors investigate the overlap of TES peroxyacyl nitrate (PAN) detections (defined as DOF>0.6) with HMS smoke extent and TES CO retrievals in the western United States. The authors 1) quantify the fraction of "enhanced" TES retrievals (DOF>0.6) overlapping HMS smoke extent by month and year, 2) perform two case studies using FRAPPE, HYSPLIT, MODIS and CALIPSO data and 3) evaluate the ratio of TES tropospheric average CO and PAN enhancements.

Based on feedback from preliminary reviews, the authors have removed comparison of TES PAN measurements with model simulations from the manuscript but have not substantially improved the quantitative characterization of the retrieved product.

We respectfully disagree with the reviewer on this point. The re-submitted version included an additional figure (Figure 1) that demonstrates the limitations in the sensitivity of TES PAN measurements.

Additionally, there are editorial and typographical errors in the manuscript (e.g., Figure 6 top panel appears almost identical to Figure S3; seemingly erroneous in text figure references – Line 178).

We have corrected the caption for Figure 7. As discussed in response to Reviewer 1, there was a mix up in reference to "black" versus "red lines" from the earlier version. Figure S3 has not been changed as we intend it to be very similar to the top panel of Figure 7 (originally Figure 6). However, S3 shows additional trajectories than the version in the main manuscript.

Further characterization of TES PAN retrievals is important and the authors have worked towards that goal.

This comment seems in contrast to the one above from this reviewer, and we assume that it refers to the addition of Figure 1, which demonstrates the limitations in sensitivity of the TES PAN measurements. Perhaps the earlier comment was written before noticing Figure 1.

However, I recommend that the authors use language that more precisely conveys the uncertainty of the product. In the introduction, for example, the authors state that "Satellite measurements [i.e., TES] are essential to understand the seasonal cycle and interannual variations of PAN (L65)."

Here and similarly throughout, use of a strong word like "Essential" connotes long-standing maturity and widespread use. In this case, I would recommend using a "potential tool" instead of "essential". While this is one specific example, edits should be made throughout the manuscript to address this concern.

We have changed the wording here as suggested and have re-read the manuscript to remove other similar instances, but the existing set of aircraft data is insufficient to identify and understand the seasonal cycle and interannual variations in PAN in the free troposphere. The one exception is the very recently collected AToM observations, and this mission has not yet ended. The specific wording has been adjusted to read:

"Given the limited set of long-term in situ measurements, satellite measurements are a potential tool that can be used to investigate the seasonal cycle and interannual variability of PAN in the troposphere along with which processes contribute to these features."

The examples below indicate where the authors can add information to the manuscript from their already accomplished analyses that will be useful to the reader.

In addition to the specific edits listed below, we have substantially increased the information in Section 2.1 in response to some suggestions by Reviewer 1. These edits add quite a bit more information about the nature of the measurements.

Figure SI 4 seems to imply that there is no statistically significant difference between "In smoke" and "Not in smoke" retrievals. Is this expected? This needs to be addressed in the main text.

This is already addressed directly in the main text in Section 3.1, but we have added a few more sentences here. This result is not surprising because the HMS smoke polygons only indicate that there is smoke in the

column. They do not indicate whether the smoke is in the free troposphere (i.e. TES can detect it) or primarily in the boundary layer, where TES has weak sensitivity. When we restrict the TES data to only those retreivals that also have elevated CO in the free troposphere (TES 510hPa CO > 120 ppbv or TES 510hPa CO > 150 ppbv), we do see a difference between the "in smoke" and "not in smoke" retrievals.

One of the paper's main findings is that ~15-32% of PAN detections (DOF > 0.6) overlap with HMS smoke extent. Is that a larger or smaller number than expected? Please report the percent of all attempted TES retrievals that overlap HMS smoke extent for context.

We have added this information to Section 3.1. This now reads: "Of all the retrievals attempted in July 2006 to July 2009, the percent associated with smoke is 18%. We expect a higher fraction of overlap in the subset of data with DOF > 0.6. This threshold value of DOF > 0.6 is consistent with a signal to noise ratio (SNR) greater than 1 (Payne et al. 2014), and this subset of data only reflects conditions with elevated PAN in the atmospheric column."

The authors report that there is no statistical difference between PAN "detections" (DOF > 0.6) that do and do not overlap HMS smoke extent. Please discuss this finding in context of past airborne or mountain-top in situ studies: should we expect there to be a statistical difference in PAN concentrations in biomass burning influenced air and other polluted airmasses.

See our response above. HMS smoke polygons only indicate that there is smoke in the column. They do not indicate whether the smoke is in the free troposphere (i.e. TES can detect it) or primarily in the boundary layer, where TES has weak sensitivity. When we restrict the TES data to only those retrievals that also have elevated CO in the free troposphere (TES 510hPa CO > 120 ppbv or TES 510hPa CO > 150 ppbv), we do see a difference between the "in smoke" and "not in smoke" retrievals. We have added several additional references to point readers to aircraft and surface measurements of PAN enhancements in biomass burning plumes. However, we note that we use aircraft data in the paper already (Figure 9). Without an enhancement in PAN above the background, our calculations would not be meaningful. Elevated PAN is often observed in biomass burning plumes.

There is one case study involving CALIPSO data. The paper might benefit from a more statistically robust analysis of CALIPSO and TES data. The meridional offset of ~500 km between the two sensor tracks (Figure 6) could likely be overcome by the incorporation of reanalysis wind products and the potentially higher quality smoke information provided by CALIPSO.

It would be interesting to do a comparison between TES and CALIPSO data, but that is beyond the scope of this paper, and would need to be focused carefully. The point of Figure 6 (now Figure 7) is to show that the smoke was likely located in the lowest 5 km of the atmosphere. We also examined CALIPSO Aerosol data from an overpass located further west on 23 July 2007. There is polluted aerosol in the column during this overpass as well. The southern portions of this overpass are located west of the active fires on this day. Similar to the image that we show in Figure 6 (now Figure 7), smoke or polluted smoke is identified from the surface to 4-5 km. The swath shown in Figure 6 overlaps an HMS smoke polygon that extends from the WA/ID border to Minnesota. We also note that the trajectories displayed in Figure 6 are based on reanalysis wind products.

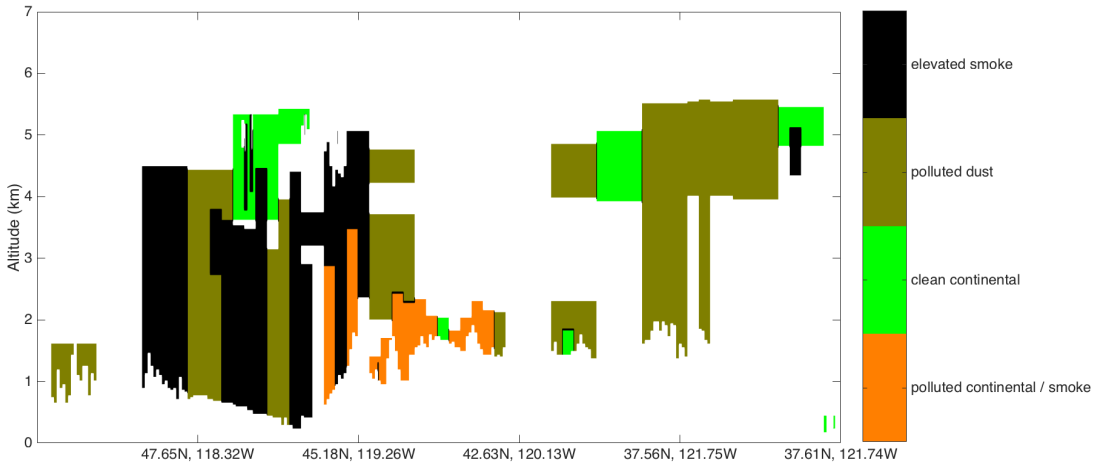

CALIPSO aerosol subtype observed on 23 July 2007, 10:23:44.5. CALIPSO Science Team (2016), CALIPSO/CALIOP Level 2, Vertical Feature Mask Data, version 4.10, Hampton, VA, USA: NASA Atmospheric Science Data Center (ASDC), Accessed by Emily V. Fischer at doi: 10.5067/CALIOP/CALIPSO/LID_L2_VFM-Standard-V4-10

"The TES PAN retrievals shown here were processed using a prototype algorithm for the area and time periods of interest." Please provide more details regarding differences between this prototype and the operational retrievals. What is the source of a priori profiles in the retrieval? What is the tropospheric average PAN concentration in the a priori profiles? The prior profile shown in Figure panel 2d shows PAN concentrations between 300 ppt and 400 ppt – if so, please justify use of an assumed "background" concentration of 100 or 200 ppt in the PAN/CO enhancement analysis in Section 3.3.

The prototype algorithm used here is effectively identical to the algorithm that has been implemented in the v7 routine Level 2 processing. We have now added further information to this effect in the text. Background PAN or CO refers to that not strongly impacted by smoke. It does not refer to the a priori.

"For footprints where the spectra show strong evidence of this silicate feature in the surface emissivity (this can occur over rocky or sandy surfaces) TES PAN retrievals are not attempted." What fraction of retrievals is discarded by this requirement? Does dust aerosol have a similar silicate absorption or emission feature that should be considered in the retrievals?

In early testing of the algorithm, we had found that desert and rocky surfaces would tend to show high initial chi-squared values for the PAN retrieval, with residual features that could only be brought within the noise by fitting strongly negative PAN VMR values. Further explanation of this issue, with a figure, is shown in Payne et al. (2014). Aside from negative values being unphysical, the current algorithm retrieves in terms of ln(vmr), so negative PAN values are not possible to retrieve within the current framework. In general, we had found that cases with high initial chi-squared values would tend to fail, and we had chosen to set a threshold (initial chi-squared > 3.0) above which retrievals are not attempted. Of course, surface emissivity features are not the only reason why there might be a high initial chi-suqared value. Another reason might be poor fits to interfering species, such as water vapor. In the current version of the algorithm, we do not attempt to explicitly track all the different reasons for failure of quality control, but instead have implemented a master quality flag. We have added the following text to address the reviewer's question about the fraction of retrievals discarded:

"Of the 28149 TES footprints processed for this work that fell over land, 3608 of them failed quality control. Concentrated regions of failed quality control show up as white patches in Figure 2(b). These regions are largely desert or mountainous regions."

The reviewer raises an interesting point about dust aerosol. There could indeed be silicate features in dust aerosol. A number of groups have looked at dust signatures in spaceborne thermal infrared radiance measurements and at their impact on other retrieval products. If the dust absorption were strong enough, this could be another reason why the TES PAN retrieval might not be attempted due to a high initial chi-squared value. If the dust absorption were sufficiently weak, this would cause the TES PAN retrieval to be biased low. A TES dust flag or dust product does not currently exist, and a rigorous assessment of the impact of dust aerosol on the TES trace gas products is outside the scope of this study, but would be worthy of consideration for future work. We have added two sentences in the manuscript on the possibility of impact from dust aerosol, with example references, and thank the reviewer for raising this point.

L118 – What is "extremely elevated"? Please quantify.
We have removed the words "extremely elevated", and this now reads:

"Mean PAN observed by the C-130 below 3 km during the field campaign was 481 pptv (Zaragoza et al., 2017). This particular day (29 July) was one of the four days identified by Zaragoza et al. (2017) with the highest surface PAN mixing ratios observed at the Boulder Atmospheric Observatory."

L130 – "We only include data with DOFS > 0.6 to ensure that the retrievals are dominated by real observed information." "Dominated" is a rather strong word to describe DOFs > 0.6. The meaning of "real observed information" is unclear.

In response to the other reviewer, we have replaced this sentence with more specific information. This now reads:

"We only include data with DOFS > 0.6. More specifically, this threshold value of DOF > 0.6 was chosen to be consistent with a signal to noise ratio (SNR) greater than 1 (Payne et al., 2014), and this criteria has been used in all the papers that have presented TES PAN data thus far (Zhu et al., 2015;Payne et al., 2016;Jiang et al., 2016;Zhu et al., 2017)."

L132 - "This conservative choice means that we are primarily basing our analysis on retrievals with high PAN" What is the mean and standard deviation of retrieved PAN concentrations?

We have added the following sentence: "The mean (standard deviation) of the retrieved tropospheric average PAN mixing ratios for DOFS > 0.6 for the region shown in the figures presented here (125^o W - 70^o W, 30^o N – 50^o N and 130^o W - 65^o W, 50^o N – 70^o N) is 0.551 (0.925) ppbv." However, this can be seen in the supplemental figures.

L172 – 193 – The purpose of this paragraph is not clear to me. Furthermore the paper evidence is not all that convincing as the expected relationships between smoke and TES PAN detections is not consistent or as expected. I did not find Figures 3 or 5 to be particularly helpful either.

The point of this paragraph is to show the spatial distribution of which TES retrievals overlap HMS smoke plumes each month. We have decided to keep all these figures in the main body of the manuscript. Figure 4 (now Figure 5) shows the distribution of tropospheric average PAN and CO as measured by TES within smoke plumes over the U.S. Figure 5 shows which day of the month overlaps a smoke plume. These figures are essential for the reader to understand the data, and the other reviewer did not make any negative comments about these figures.

L194-210 + Figure 4 – The data in this paragraph and figure can be used to compute a PAN:CO ratio that is less dependent on assumptions of background contributions. Based on a cursory visual analysis of Figure 4, a value of 0.3% PAN:CO appears reasonable. Figure 4 – The data that is "not in smoke" should be separated similarly to the data that is "in smoke." Is the relationship between CO and PAN similar "not in smoke" retrievals similar to their relationship "in smoke" (see above comment)? Should that result be expected based on previous comparisons of anthropogenic (not in smoke enhancement) and biomass burning influenced (in smoke) air?

Sure, this would be another approach, albeit a bit coarse. This quick visual approach does yield a value that agrees with many of our samples (see Figure 8 histogram). However, giving one value like this would not show the range of PAN enhancements that are observed. It does not make sense to present a PAN enhancement ratio relative to CO in non-smoke impacted samples. In these samples, the PAN and CO could have different sources. We do not know if the other samples are anthropogenically influenced. The PAN could also have been produced by lightning NO_x. Or the PAN and CO could be at different levels of the atmosphere. This is why we have been very conservative, presenting enhancement ratios only using the small subset of data where 510 hPa CO is great than 150 ppbv.

Editorial comments: Below is a non-exhaustive list of editorial suggestions or errors. I recommend that the authors thoroughly proofread before re-submission.
L1 – Re-define PAN as peroxyacyl nitrate in the body of the manuscript.

PAN is commonly known by its misnomer peroxyacetyl nitrate. This is a very minor point, and this name is used in many other manuscripts. However, we have changed the name as requested.

L140 – "infrared" [imagery]. L174 "NOAA HMA smoke plume"

Suggested change has been made.

L178 – "Supplemental Figure 1" – Perhaps intended for Supplemental Figure 2

Yes, this was also noted by Reviewer 1, and it has been corrected.

Figure S3 and Figure 6 top panel appear to be identical.

Figure S3 has not been changed as we intend it to be very similar to the top panel of Figure 7 (originally Figure 6). However, S3 shows additional trajectories than the version in the main manuscript. S3 looks a bit too cluttered for the main body of the paper, but it provides more information.

The Contribution of Fires to TES Observations of Free Tropospheric PAN over North America in July

Emily V. Fischer[1], Liye Zhu[1], Vivienne H. Payne[2], John R. Worden[2], Zhe Jiang[4], Susan S. Kulawik[3], Steven Brey[1], Arsineh Hecobian[1], Daniel Gombos[7], Karen Cady-Pereira[5], and Frank Flocke[6]

[1]Department of Atmospheric Science, Colorado State University, Fort Collins, CO, USA
[2]Jet Propulsion Laboratory, California Institute of Technology, Pasadena, CA, USA
[3]Bay Area Environmental Research Institute Moffett Field, Moffett Field, CA, USA
[4] National Center for Atmospheric Research, Boulder, CO, USA
[5] Atmospheric and Environmental Research (AER), Lexington, MA, USA
[6] National Center for Atmospheric Research (NCAR), Boulder, CO, USA
[7] MORSE Corp, Cambridge, MA, USA

Correspondence to: Emily V. Fischer (evf@atmos.colostate.edu)

Abstract. Peroxyacyl nitrate (PAN) is a critical atmospheric reservoir for nitrogen oxide radicals, and it plays a lead role in their redistribution in the troposphere. We analyze new Tropospheric Emission Spectrometer (TES) PAN observations over North America during July 2006 to 2009. Using aircraft observations from the Colorado Front Range, we demonstrate that TES can be sensitive to elevated PAN in the boundary layer even in the presence of clouds. In situ observations have shown that wildfire emissions can rapidly produce PAN, and PAN decomposition is an important component of ozone production in smoke plumes. We identify smoke-impacted TES PAN retrievals by co-location with NOAA Hazard Mapping System (HMS) smoke plumes. We find that 15 – 32 % of cases where elevated PAN is identified in TES observations (retrievals with DOF > 0.6) overlap smoke plumes. A case study of smoke transport in July 2007 illustrates that PAN enhancements associated with HMS smoke plumes can be connected to fire complexes, providing evidence that TES is sufficiently sensitive to measure elevated PAN several days downwind of major fires. Using a subset of retrievals with TES 510 hPa carbon monoxide (CO) > 150 ppbv, and multiple estimates of background PAN, we calculate enhancement ratios for tropospheric average PAN relative to CO in smoke-impacted retrievals. Most of the TES-based enhancement ratios fall within the range calculated from in situ measurements.

Emily Fischer 1/24/2018 9:47 PM
Deleted: Peroxyacetyl

1 Introduction

PAN is considered to be the largest reservoir for nitrogen oxide radicals (NO_x = NO + NO_2) in the troposphere, and it plays a major role in the redistribution of NO_x from sources to remote regions (Singh, 1987; Singh and Hanst, 1981). The balance between ozone (O_3) production and destruction is dictated by the abundance of NO_x (Monks et al., 2015), and thus the distribution of O_3 is a function of PAN production, transport, and decomposition rates (Kasibhatla et al., 1993; Moxim et al., 1996; Wang et al., 1998). However due to the complexity of its formation chemistry and its sensitivity to vertical transport (Fischer et al., 2014), PAN is difficult to represent in global chemical transport models (CTMs) (Emmons et al., 2015), and in plume scale models (Alvarado et al., 2015).

In situ observations from aircraft show rapid conversion of NO_x to PAN in smoke plumes (Alvarado et al., 2010; Müller et al., 2016) seemingly due to the oxidation of relatively short-lived non-methane volatile organic compounds (NMVOCs), particularly oxygenated species emitted in higher quantities. Elevated PAN in smoke plumes can travel significant distances (Lindaas et al., 2017), the NO_x that is eventually released can contribute to O_3 production (Bein et al., 2008; Brey and Fischer, 2016; Jaffe et al., 2013; Lindaas et al., 2017; Morris et al., 2006; Pfister et al., 2008; Singh et al., 2012), but models are unlikely to accurately predict fire-related O_3 without better incorporating the evolution of PAN in the smoke (Jaffe et al., 2013). Efforts to understand the abundance and distribution of PAN related to smoke over North America are timely because the area burned by wildfires in the western U.S. has increased in recent decades (Westerling, 2016; Westerling et al., 2006), and though there is spread in the predictions, fire activity is expected to continue to increase over the coming decades (Hurteau et al., 2014; Keywood et al., 2013; Moritz et al., 2012; Scholze et al., 2006; Yue et al., 2013). In addition, anthropogenic NO_x emissions are declining over most of North America (Pinder et al., 2008), implying that wildfires could have a greater relative impact on U.S. air quality in the future (Val Martin et al., 2015).

Aside from a handful of long term observational datasets (e.g. Brice et al. (1988); Pandey Deolal et al. (2014); Fischer et al. (2011); Tanimoto et al. (2002); Mills et al. (2007)), much of our understanding of the distribution of PAN outside urban areas rests on data from aircraft missions interpreted with global chemical transport models (Alvarado et al., 2010; Fadnavis et al., 2014; Fischer et al., 2014; Pope et al., 2016). Given the limited set of long-term in situ measurements, satellite measurements are a potential tool that can be used to investigate the seasonal cycle and interannual variability of PAN in the troposphere along with which processes contribute to these features. Limb-sounding satellite instruments have provided global distributions of PAN in the upper troposphere and lower stratosphere (Glatthor et al., 2007; Moore and Remedios, 2010; Ungermann et al., 2016; Wiegele et al., 2012). Analysis of new observations of PAN from the Tropospheric Emission Spectrometer (TES) can be used to look lower in the troposphere (Payne et al., 2014). TES PAN observations confirm the important role that high latitude fires play in the interannual variability of PAN during spring at high latitudes (Zhu et al., 2015), support estimates of the role of PAN in the transpacific transport of O_3 (Jiang et al., 2016), establish strong intercontinental transport of PAN in both spring and summer (Zhu et al., 2017), and provide confirmation of PAN features

Emily Fischer 2/13/2018 10:56 AM
Deleted: ,

Emily Fischer 2/11/2018 4:55 PM
Comment [1]: Citations have been updated to include Fadnavis et al. (2014) and Pope et al., (2016)

Emily Fischer 1/19/2018 3:53 PM
Deleted: essential

Emily Fischer 1/19/2018 3:53 PM
Deleted: to

Emily Fischer 1/19/2018 3:53 PM
Deleted: understand the

Emily Fischer 2/11/2018 4:55 PM
Comment [2]: Citations have been updated to include Ungermann et al. (2016)

in the tropics predicted by CTMs (Payne et al., 2016). TES retrievals have also shown elevated PAN in smoke plumes over North America (Alvarado et al., 2011).

Here we present an analysis of TES PAN observations over North America during the month of July between 2006 and 2009. We focus on understanding the contribution of smoke to enhanced PAN by segregating TES PAN retrievals based on smoke-impact through comparisons to NOAA Hazard Mapping System (HMS) smoke plumes.

2 Methods

2.1 TES PAN observations

TES is a nadir-viewing Fourier transform spectrometer that measures thermal infrared radiances at a high spectral resolution (0.1 cm^{-1} apodized), and it is one of four instruments on the NASA Aura satellite, which flies in a sun-synchronous orbit with local equator crossing times of 1:30 and 13:30. TES has a number of observational modes (global survey, and special observation modes such as step-and-stare and transect). In global survey mode TES makes measurements along the satellite track for 16 orbits with a spacing of ~200 km; in step-and-stare mode nadir measurements are made every 40 km along the track for approximately 50 degrees of latitude; in transect mode observations consist of series of 40 consecutive scans spaced 12 km apart.

Specific details of the TES PAN retrieval algorithm are provided in Payne et al. (2014). TES PAN retrievals are being processed routinely for the whole TES dataset and are publicly available in the TES v7 Level 2 product. The retrievals use an optimal estimation approach (Bowman et al., 2006; Rodgers, 2000). An important diagnostic output of the optimal estimation retrieval is the averaging kernel (**A**) which describes the sensitivity of the retrieval to the true state:

(1) $A = \frac{\partial \hat{x}}{\partial x} = (K^T S_n^{-1} K + R)^{-1} K^T S_n^{-1} K = GK$

The Jacobian (**K**) is the sensitivity of the forward modeled radiances to the state vector, calculated as:

(2) $K = {}^{\partial L}/_{\partial \hat{x}}$

The noise covariance matrix, $\mathbf{S_n}$, represents the noise in the measured radiances. **R** is the constraint matrix for the retrieval. The averaging kernel matrix is supplied for each individual TES measurement. The retrieved state is related to the true state by the following equation:

(3) $\hat{x} = x_a + A(x - x_a) + G_\varepsilon$

This allows us to apply the averaging kernel to a reference profile, such as an aircraft profile measurement, to evaluate what the TES retreival would show if the reference profile represents the true atmospheric state viewed from the satellite.

At the time of this work, the v7 product was not yet available. The TES PAN retrievals shown here were processed using a prototype algorithm for the area and time periods of interest. The v7 PAN algorithm was built from this prototype, using the same state vector representation, microwindows and prior constraints. The *a priori* profiles are based on GEOS-Chem simulations for the year 2008, with 6 possible prior profiles for any given month, as described in Payne et al. (2014). We have verified, using a subset of v7 data processed so far, that v7 retrievals are consistent with those from the prototype. On a

Emily Fischer 2/13/2018 10:57 AM
Formatted: Font:Bold

Emily Fischer 2/11/2018 4:56 PM
Deleted: An important diagnostic output of the optimal estimation retrieval is the averaging kernel, A, which describes the sensitivity of the retrieval to the true state:

Emily Fischer 2/11/2018 4:57 PM
Formatted: Indent: First line: 0"

Emily Fischer 2/11/2018 5:03 PM
Formatted: Font:Bold

Emily Fischer 2/11/2018 5:03 PM
Formatted: Font:Bold

Emily Fischer 2/11/2018 5:03 PM
Formatted: Font:Bold, Subscript

Emily Fischer 2/11/2018 5:03 PM
Formatted: Font:Bold

Emily Fischer 2/11/2018 5:03 PM
Deleted: $\mathbf{x_{hat}} = \mathbf{x_a} + \mathbf{A(x-x_a)+Gε}$.
AA

Emily Fischer 2/11/2018 5:05 PM
Formatted: Font:Times New Roman

Emily Fischer 2/11/2018 5:05 PM
Deleted: A

Emily Fischer 2/11/2018 5:06 PM
Formatted: Font:Italic

Emily Fischer 2/11/2018 5:05 PM
Deleted: . The v7 PAN algorithm was built from this prototype, using the same state vector representation, microwindows and prior constraints. The a priori profiles are based on GEOS-Chem simulations for the year 2008, with 6 possible prior profiles for any given month, as described in Payne et al. [2014]. We have verified, using a subset of v7 data processed so far, that v7 retrievals are consistent with those from the prototype.

single footprint basis, TES is capable of measuring elevated PAN (detection limit ~ 0.2 ppbv) in the free troposphere, with uncertainty of 30-50 %. In order to illustrate the characteristics of the retrievals, the four panels in Figure 1 show simulated retrievals for different combinations of conditions. The true profiles in Figure 1 are the profiles that were used to generate radiances and Jacobians for the purposes of the simulated retrievals shown in the Figure. The true profile exhibits a maximum in the PAN mixing ratio close to the surface in the upper panels (a and b), while the true profile peaks in the mid-troposphere in the lower panels (c and d). In each of the profile plots, the black dashed line shows the prior, the two red lines show two different true profiles, and the two blue lines show the retrieved profiles. In order to demonstrate the reduction in lower tropospheric sensitivity associated with cloudy cases, panels on the right (b and d) show retrievals where a cloud with effective optical depth of 0.7 is placed at 600 hPa (dotted line). These can be directly compared with panels on the left (a and c), which show equivalent condition clear-sky retrievals. As discussed in Payne et al. (2014), the TES PAN retrievals do not provide information on the vertical variation of PAN. In all cases, the degrees of freedom for signal, or number of independent pieces of vertical information in the retrieval, is less than 1.0. This means that the shape of the retrieved result is always influenced by the shape of the prior (black dashed line), as can be seen in this Figure, and the vertical distribution of PAN in each retrieval is uncertain. Figure 1 demonstrates the limitations in sensitivity of TES PAN measurements, which provide broader spatial and temporal coverage than in situ measurements, but with a compromise on sensitivity. However, the measurements can be used to validate models, provided the averaging kernel and prior are applied to model fields before comparison with the retrievals. The averaging kernels associated with the panels presented in Figure 1 are provided in the Supplemental Information (Figure S1).

Figure 2 shows the July 2006 – 2009 tropospheric average PAN. Because of the lack of vertical information, we define the tropospheric average for a given retrieval as the average retrieved PAN between 800 hPa and the tropopause. The PAN spectral feature at 1140-1180 cm^{-1} used for the TES retrievals coincides with the location of a silicate feature in surface emissivity spectra. For footprints where the spectra show strong evidence of this silicate feature in the surface emissivity (this can occur over rocky or sandy surfaces), TES PAN retrievals are not attempted. Of the 28149 TES footprints processed for this work that fell over land, 3608 of them failed quality control. Spatially coherent regions of failed quality control show up as white patches in Figure 2(b). These regions are largely desert or mountainous regions. The same silicate feature is present in the presence of dust aerosol (*e.g.,* DeSouza-Machado et al. (2006); Klüser et al. (2011); Capelle et al. (2014). The presence of dust aerosol could therefore also cause the retrieval to fail quality control or, for more subtle cases, could lead to low-biased PAN retrievals. Other reasons that may cause the TES PAN retrieval to fail quality control include poor fits to interferents, such as water vapor, within the PAN spectral range.

When all the existing TES data is gridded (Figure 2b), there are several large patterns that emerge. 1) Average tropospheric PAN mixing ratios in the TES observations generally increase with latitude during the month of July over North America. 2) Average tropospheric PAN mixing ratios generally decrease

Microsoft Office User 2/6/2018 12:37 AM
Deleted: The PAN spectral feature at 1140-1180 cm^{-1} used for the TES retrievals coincides with the location of a silicate feature in surface emissivity spectra. For footprints where the spectra show strong evidence of this silicate feature in the surface emissivity (this can occur over rocky or sandy surfaces), TES PAN retrievals are not attempted.

Emily Fischer 2/11/2018 5:07 PM
Deleted: are the profiles that were used to generate radiances and jacobians for the purposes of the simulated retrievals shown in the Figure

Microsoft Office User 2/3/2018 10:26 AM
Deleted: heavily

Emily Fischer 2/13/2018 10:57 AM
Deleted: figure

Emily Fischer 2/13/2018 10:57 AM
Formatted: Indent: First line: 0.5"

from west to east. 3) As can be seen in later figures, there are relatively few retrievals per grid box over the southwestern U.S. Though there are relatively few samples (~5-20 per 2x2°grid box), relatively high mixing ratios (0.6 ppbv) are observed over the Colorado Front Range.

The peak sensitivity for PAN is generally between 400 – 800 hPa (Payne et al., 2014), but a comparison between TES PAN transect observations coincident with Front Range Air Pollution and Photochemistry Éxperiment (FRAPPÉ) observations (Figure 3) show that TES can have some degree of sensitivity to PAN in the boundary layer when boundary layer PAN is elevated. As an example, Figure 3 presents in situ observations from a flight during FRAPPÉ made with a thermal dissociation chemical ionization mass spectrometer (TD-CIMS) (Zheng et al., 2011). Mean PAN observed by the C-130 below 3 km during the field campaign was 481 pptv (Zaragoza et al., 2017). This particular day (29 July) was one of the four days identified by Zaragoza et al. (2017) with the highest surface PAN mixing ratios observed at the Boulder Atmospheric Observatory. The overlaid TES data in Figure 3a (parallelograms) show an enhancement in the TES PAN (as shown by the TES observation highlighted by a black square) in the vicinity of aircraft measurements of highly elevated PAN values in the boundary layer indicating that in this case TES is weakly sensitive to the elevated boundary layer values despite the presence of high clouds (dashed line Figure 3c). Figure 3 also shows red and blue lines corresponding to application of the averaging kernel for this case to hypothetical "true" profiles with and without the enhancement in the boundary layer. The red and blue lines show that TES has some sensitivity to PAN below 800 hPa, but the retrieval places the additional PAN higher up in the atmosphere. While the difference between the red and the blue solid lines in Figure 3d is small, it is non-zero indicating that TES has some sensitivity to the boundary layer enhancement in this case.

For the analysis presented below, we use PAN observations from TES over North America in July, from 2006 to 2009. We only include data with DOFS ≥ 0.6. More specifically, this threshold value of DOF > 0.6 was chosen to be consistent with a signal to noise ratio (SNR) greater than 1 (Payne et al., 2014), and this criteria has been used in all the papers that have presented TES PAN data thus far (Jiang et al., 2016; Payne et al., 2016; Zhu et al., 2017; Zhu et al., 2015). This conservative choice means that we are primarily basing our analysis on retrievals with high PAN. The mean (standard deviation) of the retrieved tropospheric average PAN mixing ratios for DOFS > 0.6 for the region shown in the figures presented here (125° W - 70° W, 30° N – 50° N and 130° W - 65° W, 50° N – 70° N) is 0.55 (0.93) ppbv. The impact of this choice can be seen when we compare the PAN distribution observed by TES under different conditions later in Section 3.2

2.2 NOAA Hazard Mapping System (HMS) Smoke Plume Extent

We segregate the TES PAN retrievals by whether or not the TES footprint coincides with a smoke plume identified by the NOAA Hazard Mapping System (HMS). NOAA HMS is an interactive satellite image and graphics system developed by the National Environmental Satellite, Data, and Information Service (NESDIS). Using satellite imagery, trained analysts identify the geographic extent of smoke-plumes in the atmospheric column over North America (Rolph et al., 2009; Ruminski et al., 2006). Visible-

Emily Fischer 2/13/2018 10:58 AM
Deleted:

Emily Fischer 2/13/2018 10:58 AM
Deleted: 2

Emily Fischer 1/24/2018 8:55 PM
Deleted: is extremely elevated

Emily Fischer 1/19/2018 3:09 PM
Deleted: 2

Emily Fischer 1/24/2018 9:01 PM
Deleted: In situ data show mixing ratios up to 2.2 ppbv were observed within the boundary layer. Afternoon mixing ratios > 1 ppbv were also observed at the Boulder Atmospheric Observatory (BAO) ground site on this day (Zaragoza et al., 2017).

Emily Fischer 1/19/2018 3:09 PM
Deleted: 2a

Microsoft Office User 2/3/2018 11:37 AM
Deleted: show

Emily Fischer 1/19/2018 3:09 PM
Deleted: 2c

Emily Fischer 1/19/2018 3:09 PM
Deleted: 2

Microsoft Office User 2/3/2018 11:44 AM
Deleted:

Emily Fischer 1/19/2018 3:09 PM
Moved (insertion) [1]

Microsoft Office User 2/3/2018 11:35 AM
Deleted: T

Emily Fischer 1/19/2018 3:10 PM
Deleted:

Microsoft Office User 2/3/2018 11:35 AM
Deleted: es

Emily Fischer 1/19/2018 3:10 PM
Deleted:

Microsoft Office User 2/3/2018 11:44 AM
Deleted: This is also what is plotted in Figure 2a 2 and used throughout the paper.

Emily Fischer 2/13/2018 10:58 AM
Formatted: No underline

Emily Fischer 1/24/2018 9:04 PM
Deleted: to ensure that the retrievals are dominated by real observed information rather than the *a priori*.

band geostationary (~15 minute refresh rate) imagery, occasionally assisted by infrared imagery, is used to detect smoke plumes in the atmospheric column (Ruminski et al., 2006); because smoke plumes are primarily identified with visible imagery, the analyzed smoke plume extent is only representative of local daylight hours.

Plumes are analyzed multiple times on a given day and can be nested. For this work all overlapping plumes (either nested or analyzed at different times) are merged into a single plume. This dataset does not contain information about the vertical location or depth of smoke in the atmospheric column. As discussed in Brey et al. (2017), the number and extent of smoke plumes in this HMS dataset is a conservative estimate. In particular, it becomes challenging to identify smoke as it dilutes during transport or mixes with anthropogenic haze. Thus our estimate of the number of PAN retrievals impacted by smoke may be a lower bound. For this work, we follow the overlap methods described in Brey et al. (2017). We matched all TES PAN retrievals based on UTC day. This means that overnight retrievals are paired with the plume from the prior day. As discussed in Brey et al. (2017), most of the large wildfire plumes occurring in July over the western U.S. are very large and last several days. So we would expect that pairing the overnight retrievals with the plume from the prior day (i.e. matching based only on UTC day) is not likely to change our results, and that is the case. We have repeated all our calculations using only the daytime retrievals, and the choice to use all the retrievals does not change the results.

2.3 HYSPLIT trajectories

As part of a case study presented in Section 3.3, we use the Hybrid Single-Particle Lagrangian Integrated Trajectory (HYSPLIT) model (Draxler, 1998) (http://ready.arl.noaa.gov/HYSPLIT.php) to simulate the air mass history of a subset of TES PAN retrievals associated with relatively fresh (0 – 2 days of atmospheric processing) smoke. HYSPLIT has been used extensively to model the transport of smoke (*e.g.*, Stein et al. (2015) and Brey et al. (2017)). For this application, the HYSPLIT model is driven by global meteorological data from the Global Data Assimilation System (GDAS) archive (ftp://arlftp.arlhq.noaa.gov/pub/archives/gdas1). GDAS has a time step of 3-hours, horizontal grid spacing of 1^{o} latitude by 1^{o} longitude (~120 km), and 23 pressure surfaces between 1000 and 20 hPa (Kanamitsu, 1989). We initialized 5-day backward trajectories for set of single TES retrievals at the retrieval times and locations. In the case study in Section 3.3 we used trajectories initialized at 2, 4 and 6 km above ground level (agl). As the vertical distribution of PAN in each retrieval is uncertain (Section 2.1), we calculated backward trajectories using these three altitudes to test the sensitivity of our results to the choice of initialization altitude.

3 Results

3.1 North American TES PAN Retrievals Associated with Smoke

The first four panels of Figure 4 show the spatial distribution of TES PAN retrievals over the U.S. and southern Canada for the month of July 2006 to 2009. All retrievals plotted in this figure have DOF > 0.6. The retrievals are colored red when they fall within a NOAA HMA smoke plume. A large fraction of the TES retrievals (15-32%) during this month overlap smoke plumes; the largest percentage of retrievals

Emily Fischer 1/19/2018 3:26 PM
Deleted: 3

associated with smoke occurred in July 2008 (32%), though this year does not display a high percentage of detection compared to other years and the average tropospheric PAN measured by TES is not larger than other years (Supplemental Figure 2). Of all the retrievals attempted in July 2006 to July 2009, the percent associated with smoke is 18%. We expect a higher fraction of overlap in the subset of data with DOF > 0.6. This threshold value of DOF > 0.6 is consistent with a signal to noise ratio (SNR) greater than 1 (Payne et al. 2014), and this subset of data only reflects conditions with elevated PAN in the atmospheric column. The number of major wildfires over the U.S. has large seasonal and interannual variability (Brey et al., 2017). Wildfires in summer 2008 were particularly intense over California associated with record-breaking lightning and aggravated drought. Figure 4c shows a cluster of TES PAN retrievals over California associated with this smoke. The dense smoke, which spread substantially downwind, was sampled from the NASA DC-8 aircraft as part of the Arctic Research of the Composition of the Troposphere from Aircraft and Satellites (ARCTAS-CARB) campaign (Hecobian et al., 2011; Singh et al., 2010; Singh et al., 2012), and we show this data in Section 3.3. Elevated smoke was also observed at surface sites downwind throughout the month of July (Gyawali et al., 2009). As part of ARCTAS-B, Alvarado et al. (2010) also documented major PAN enhancements in fresh wildfire plumes sampled over Canada during July 2008. July 2008 was also associated with special observations from TES, providing a relatively high number of attempted retrievals this month (red line in Supplemental Figure 2). Figure 4f presents the seasonal transition for 2006 in smoke-plume polygon overlap from late spring (May) to early autumn (September). During this example year, the percentage of TES PAN retrievals with DOF > 0.6 associated with smoke peaked in July (20%), but Figure 4e suggests that this was not a notably high percentage of smoke-impacted retrievals. A much higher percentage of DOF > 0.6 retrievals were smoke-impacted in July 2008.

Panels a and b of Figure 5 show the distribution of tropospheric average TES PAN in the subset of retrievals overlapping HMS smoke plume polygons in July 2006-2009. The distributions of tropospheric PAN in the subset of retrievals with DOF ≥ 0.6 is not different between the in-smoke cases (leftmost red box plot in Figure 5a) and the not-in-smoke cases (Blue-Grey box plot in Figure 5a). The choice to only include data with DOFS ≥ 0.6, pushes the median tropospheric average PAN substantially higher than using all the available TES data. Thus the percent of retrievals impacted by smoke shown in Figure 4 reflects only situations with substantially elevated PAN in the atmospheric column. Imposing an additional cloud optical depth filter does not substantially change the distribution of tropospheric average PAN (see Supplemental Figure 4). The other two red distributions in Figure 5a reflect additional criteria designed to ensure that the PAN associated with smoke in the atmospheric column exists in the free troposphere where we expect TES to be most sensitive. We show the PAN distribution for in-smoke cases that also coincide with TES 510hPa CO > 120 ppbv and TES 510hPa CO > 150 ppbv. There are differences between these subsets of data and the not-in smoke cases. As discussed further in Section 3.3, background CO in July in the northern mid-latitudes is expected to be ~85 ppbv. Both criteria (510 hPa CO > 120 ppbv or 510 hPa CO > 150 ppbv) represent conservative indicators of smoke in the free troposphere. The latter subset is

Emily Fischer 1/19/2018 3:17 PM
Deleted: 1

Emily Fischer 1/19/2018 4:23 PM
Formatted: Font:Not Italic

Emily Fischer 1/19/2018 3:26 PM
Deleted: 3a

Emily Fischer 1/19/2018 3:31 PM
Deleted: 3f

Emily Fischer 1/19/2018 3:31 PM
Deleted: 3e

Emily Fischer 1/19/2018 3:31 PM
Deleted: 4

Emily Fischer 2/13/2018 10:59 AM
Formatted: No underline

Emily Fischer 1/19/2018 3:31 PM
Deleted: 4a

Emily Fischer 1/19/2018 3:31 PM
Deleted: 4a

Emily Fischer 2/13/2018 10:59 AM
Formatted: No underline

Emily Fischer 1/19/2018 3:31 PM
Deleted: 3

Emily Fischer 1/19/2018 3:31 PM
Deleted: 4a

shown because this designation has been used previously (Alvarado et al., 2011), and we use this subset in our calculation of enhancement ratios in Section 3.3.

Figure 5c and 5d present the distribution of tropospheric mean CO associated with the successful PAN measurements. There is higher CO associated with TES retrievals that overlap HMS smoke polygons (median = 100 ppbv versus 92 ppbv for both day and night retrievals), and the upper tail of the CO distribution includes retrievals with tropospheric average CO above 200 ppbv. The difference in CO distributions in and out of smoke provides confidence in the use of the HMS smoke product as a smoke-impact filter. The tropospheric average CO distributions are shown for reference because we combine tropospheric average CO with tropospheric average PAN to calculate PAN enhancement ratios in Section 3.3. There are several other factors that may also contribute to the patterns shown in Figure 5 that are worth noting. In general, TES is more sensitive to CO than PAN in the lowermost atmosphere, and the HMS smoke product, which contains no vertical information, includes smoke plumes near the surface and higher in the column. Though the sensitivity to clouds appears to be modest in our data, the TES CO retrievals are even less sensitive overall to the presence of cloud than the TES PAN retrievals. Third, many of the smoke-impacted TES retrievals are located substantially downwind of the source fires. PAN has a substantially shorter lifetime than CO in the warm lower atmosphere in summer.

3.2 July 2007 Case Study

TES observations allow measurements of smoke plumes over North America at various ages, even in the same day. Figure 6 shows the spatial distribution of TES retrievals with DOF > 0.6 over the U.S. and southern Canada for the month of July 2006 to 2009 that overlapped HMS smoke plume polygons. These points are the red colored retrieval locations in Figure 4, but here they have been colored by the day of the month. The filled dots represent points where TES 510 hPa CO > 150 ppbv, and these are the points used to calculate PAN enhancement ratios in Section 3.3. The presence of same colored dots demonstrate that wide swaths of North America can have smoke located somewhere in the atmospheric column on a given day, and that the smoke is associated with elevated PAN (> 200 pptv) in the atmospheric column. As discussed in Brey et al. (2017), smoke plumes vary in size substantially. Small plumes cover < 100 km^2 and smoke plumes from major fire complexes can spread over several Western States or entire Canadian Provinces. For example, Figure 6 shows elevated PAN both directly over and east of Hudson Bay in late July 2008 associated with fires in northern Saskatchewan.

Next we present a case study of fires in Idaho and Montana during July 2007 that connects PAN enhancements associated with HMS smoke plumes to regions impacted by fires, indicating that the TES sensitivity is often sufficient to measure elevated PAN several days downwind of a fire. Figure 7 presents the locations of TES retrievals with elevated (DOF > 0.6) PAN on 22 and 23 July 2007, red and purple dots respectively, along with FIRMS MODIS hotspots (Giglio et al., 2006; Giglio et al., 2003) on those two dates. The TES PAN retrievals are located almost directly over active fires in Idaho on 22 July, but this does not absolutely ensure that the PAN is from fresh smoke. As discussed in Payne et al. (2014), TES is most sensitive to PAN in the mid-troposphere, and we do not have injection height information for these

Emily Fischer 1/19/2018 3:32 PM
Deleted: 4c

Emily Fischer 1/19/2018 3:32 PM
Deleted: 4d

Emily Fischer 1/19/2018 3:32 PM
Deleted: 4

Emily Fischer 1/19/2018 3:32 PM
Deleted: 5

Emily Fischer 1/19/2018 3:32 PM
Deleted: 3

Emily Fischer 1/19/2018 3:32 PM
Deleted: 5

Emily Fischer 1/19/2018 3:32 PM
Deleted: 6

Emily Fischer 2/13/2018 10:59 AM
Formatted: Font:Not Italic

Emily Fischer 2/13/2018 10:59 AM
Deleted: [

Emily Fischer 2/13/2018 10:59 AM
Deleted:]

specific fires. The TES PAN retrievals on 23 July (located over rural areas in North and South Dakota) are not located directly over active fires, but they do overlap HMS smoke polygons. The purple lines show HYSPLIT backward trajectories initialized from 4 km at the locations of the retrievals on 23 July. The trajectories show that the major fire complexes in Idaho and Montana likely contributed to the smoke observed by TES on 23 July (purple dots). If so, this smoke was approximately 1-2 days old at the time of the retrieval. The trajectories show that the smoke observed over South Dakota is likely older (2-3 days of atmospheric aging). We initialize the trajectories from various heights (2, 4 and 6 km) because the TES PAN retrievals offer no vertical information, and all these trajectories are plotted in Supplemental Figure S3. The smoke filled a relatively thick layer based on available CALIPSO data. A CALIPSO overpass on 23 July 2007 (lower panel of Figure 7) shows an aerosol layer identified largely as *elevated smoke* extending from the surface to ~5 km over this region.

3.3 PAN Enhancements in North American Biomass Burning Plumes

Enhancement ratios relative to CO or another tracer (e.g. acetonitrile for biomass burning specifically) are a common way to characterize the composition of pollution plumes (Yokelson et al., 2013). Enhancement ratios are calculated from samples made from within and outside a given plume (i.e. background air). This section presents enhancement ratios calculated from TES PAN retrievals located within smoke plumes. We show that the tropospheric PAN enhancement ratios from TES fall within the range of relevant aircraft measurements over North America. We also show that there are many pitfalls associated with using enhancement ratios as observed from TES to study the evolution of PAN in the smoke plumes we have identified here.

Equation 4 indicates how the enhancement ratio of PAN relative to CO is calculated here.

$$(4)\ PAN_{ER} = \frac{(PAN_{plume} - PAN_{background})}{(CO_{plume} - CO_{background})}$$

Figure 8 presents a histogram of PAN enhancement ratios in the subset of retrievals that overlap HMS smoke polygons and also are likely to have elevated PAN and CO in the free troposphere (TES CO > 150 hPa). The purple dots designate the two retrievals shown in Figure 7 that meet these strict criteria. PAN enhancement ratios were estimated using tropospheric average PAN and tropospheric average CO. We performed this calculation using Equation 4 and a CO background of 80 and 90 ppbv. Background CO in the Northern Hemisphere is generally between 80 and 90 ppbv (*e.g.* Parrish et al. (1991)) with significant year-to-year variability largely driven by boreal forest fire emissions (Wotawa et al., 2001). Thus the lower mixing ratio (80 ppbv) is closer to estimates of background CO in the Northern Hemisphere. The upper mixing ratio (90 ppbv) reflects the median tropospheric average CO (91 ppbv) in the PAN TES retrievals not overlapping HMS Smoke Polygons (blue-grey points in Figure 4). Though we repeated this calculation with various assumptions of background CO mixing ratios, this choice does not impact the major key point we draw from Figure 8. Even with our conservative CO criteria applied, the TES PAN data offer the opportunity to calculate tropospheric average PAN enhancements relative to CO for a large number of smoke samples (N =159) over a variety of regions and distances downwind from fires. The median PAN enhancement ratio relative to CO calculated using a background PAN mixing ratio of 0.1 ppbv and a

Emily Fischer 2/13/2018 10:59 AM
Deleted: e

Emily Fischer 1/19/2018 3:32 PM
Deleted: 6

Emily Fischer 1/16/2018 4:33 PM
Formatted: Font:Not Italic

Emily Fischer 1/16/2018 4:33 PM
Formatted: Font:Not Italic

Emily Fischer 1/16/2018 4:33 PM
Formatted: Indent: First line: 0"

Emily Fischer 1/19/2018 3:33 PM
Deleted: 7

Emily Fischer 1/19/2018 3:36 PM
Deleted: shown in Figure 7 (colored dots), as well as these values for the entire suite of retrievals

Emily Fischer 1/19/2018 3:33 PM
Deleted: 3

Emily Fischer 1/19/2018 3:33 PM
Deleted: 7

background CO mixing ratios of 90 ppbv is 0.43 %. When we assume a higher PAN background mixing ratio of 0.2 ppbv with this background CO mixing ratio, the median PAN enhancement ratio from the TES data is 0.29 %. As we show next, these values are similar to that reported from in situ measurements.

We have not been able to identify a case study where the TES data can be used to examine the evolution of the enhancement ratio of PAN relative to CO in a plume. Restricting ourselves to the conservative criteria of 510 hPa CO > 150 ppbv severely reduces the sample size (from 1151 to 159). In addition, the 5 km x 8 km footprint of TES combined with the lack of vertical sensitivity makes it difficult to establish the age of the smoke contributing to the enhanced PAN and CO. There could be multiple layers of smoke in the column, of various ages. Tracking plumes with aircraft allows for a more precise determination of plume age. In addition, PAN does not simply dilute proportionally to CO because its dissociation is also a function of temperature, which also depends on altitude.

We compare the TES column PAN enhancement ratios to enhancement ratios of PAN relative to CO observed during July 2008 during the ARCTAS/CARB field campaign (Hecobian et al., 2011). Smoke identification within the aircraft dataset is discussed in detail in Hecobian et al. (2011) and not repeated here. Alvarado et al. (2010) report mean PAN enhancement ratios for boreal plumes using this same dataset. They report enhancement ratios of 0.34 ± 0.35 % (range = 0.09 % to 1.43 %) for fresh plumes and 0.28 ± 0.36 % (range = 0.16 % to 0.68 %) for old plumes. In Alvarado et al. (2010), fresh plumes were designated as those where propene was correlated with CO, and aged plumes were designated as plumes where CO was correlated with more long-lived species, like butane, benzene and propane. The enhancement ratios were calculated using aircraft data from plume crossings using the average within-plume PAN and CO mixing ratios and assuming background mixing ratios equal to the 25th percentile of all measurements in the boundary layer (140 ppbv for CO and 180 pptv for PAN). To calculate enhancement ratios presented in Figure 9, we used the 25th percentile for each trace gas for each day. For simplicity, we used observations at all altitudes, not just boundary layer points. Figure 9 shows that there is a range of in situ enhancement ratios. Similar to the tropospheric average enhancement ratio from TES, the majority of these enhancement ratios fall below 1%. There are retrievals with PAN enhancement ratios greater than 1%, but the number of these depends on the assumed background PAN used in the calculation. The appropriate value to use is difficult to determine from the TES data alone, which is why a range of estimates is presented in Figure 8. Figure 9 presents enhancement ratios calculated from in situ measurements. This data shows that there is a higher median enhancement for plumes from fires in the northwestern U.S., than the boreal plumes, though there are vastly different numbers of samples.

A second chance for a qualitative comparison of PAN enhancement ratios in smoke plumes is presented in Briggs et al. (2016); summertime observations of 23 different plumes from the Mount Bachelor Observatory indicate PAN enhancement ratios of 1.46 – 6.25 pptv ppbv^{-1} (0.146 – 0.625 %). This range overlaps with the majority of the column average enhancement ratios from TES. All of the plumes identified in Briggs et al. (2016) were from fires in northern California or southeastern and central Oregon, so they differ from the fires intercepted during ARCTAS.

Emily Fischer 1/19/2018 3:33 PM
Deleted: 8

Emily Fischer 1/19/2018 3:33 PM
Deleted: 8

Emily Fischer 1/19/2018 3:33 PM
Deleted: 7

Emily Fischer 1/19/2018 3:33 PM
Deleted: 8

4.0 Conclusions

We present the first detailed analysis of TES PAN measurements over North America. Recent aircraft observations over Colorado offer the most direct overlap of the TES PAN product with in situ aircraft observations to date. This comparison indicates that TES can be sensitive to PAN in the boundary layer when PAN in the boundary layer is elevated, though peak sensitivity is in the free troposphere. We use a period with a large number of TES PAN observations (2006 – 2009) to investigate the contribution of fire smoke to elevated PAN over North America in July. This type of multi-year synthesis is not possible with any other observational dataset, and demonstrates how satellite measurements of PAN can be used to frame new questions that cannot be answered with existing in situ measurements.

1. We segregate and examine the abundance of tropospheric average PAN relative to CO in TES retrievals located within smoke plumes identified by the NOAA Hazard Mapping System (HMS). We find that a large fraction of the TES retrievals (15-32%) during the month of July overlap smoke plumes during the period 2006 – 2009, while the largest percentage of retrievals associated with smoke occurred in July 2008 (32%). Tropospheric average CO is clearly enhanced in retrievals impacted by smoke, but a difference in PAN between smoke-free and smoke-impacted retrievals is insignificant.

2. We compare the tropospheric average PAN enhancement relative to CO in smoke-impacted samples and find that our satellite-based estimates largely fall within the range of enhancement ratios that have been observed from recent aircraft and surface campaigns over western North America. While in situ measurements represent samples from a select number of plumes, the satellite measurements offer more samples of different plumes and observations over regions and time periods that have not been sampled by aircraft.

3. We use a case study to illustrate that PAN enhancements associated with HMS smoke plumes can be connected to regions impacted by fires, indicating that the TES sensitivity is often sufficient to measure elevated PAN several days downwind of a fire.

4. Case studies of specific smoke events do not show a systematic pattern in PAN enhancements relative to CO as a function of distance downwind from presumed source fires. We also do not observe any consistent evolution in the PAN enhancement ratio when this calculation is done using the tropospheric maximum PAN and CO from the TES retrievals, rather than the tropospheric averages. The TES PAN data are not useful in this context because of large limitations associated with evaluating smoke age within the TES data.

PAN is considered to be the most important reservoir for NO_x in the troposphere, and it plays a critical role in the redistribution of NO_x to remote regions. The work presented here highlights the importance of fires as a source of PAN over North America in summer. It also shows that TES measurements of PAN can be used to complement limited in situ measurements of PAN. The apparent significant contribution of fires to elevated PAN plumes over North America underscores the importance of investigating PAN production in smoke to ultimately determine the best way to incorporate the rapid

chemistry that produces PAN into chemical transport models that are used to predict background O_3 and exceptional O_3 events.

Data Availability: TES PAN retrievals are being processed routinely for the whole TES dataset and will be publicly available in the TES v7 Level 2 product. However, at the time of submission, the v7 processing is still underway. For netCDF files containing TES PAN data used in this study, please contact Dr. Vivienne H. Payne at Vivienne.H.Payne@jpl.nasa.gov. When the paper is accepted for final publication, we will add a text file containing the latitude, longitude, time, HMS smoke overlap status, and tropospheric average PAN and CO to the CSU digital repository (http://hdl.handle.net/10217/180136) we have already established.

Appendices: N/A

Supplemental Information: Uploaded as a separate PDF.

Team List and Author Contributions:

Emily V. Fischer led the majority of the analysis and writing associated with this manuscript.

Liye Zhu provided basic statistical analyses of the TES data for the region of interest.

Vivienne H. Payne led the processing and development of the TES PAN data.

John R. Worden provided guidance on the use of the TES PAN data.

Zhe Jiang provided guidance on the use of the TES PAN data.

Susan S. Kulawik supported the algorithm development for the TES PAN retrieval.

Steven Brey led the overlap analysis of the TES retrievals with HMS smoke plumes.

Arsineh Hecobian provided the smoke designation associated with the ARCTAS aircraft data.

Dan Gombos and Karen Cady-Pereira performed data analysis and visualization of TES PAN distributions, concentrations, and averaging kernels from the FRAPPE aircraft and satellite data

Frank Flocke was responsible for the FRAPPE aircraft PAN measurements.

Competing interests: The authors declare that they have no conflict of interest.
Disclaimer: N/A

Special issue statement: N/A

Acknowledgements. This work was supported by NASA Award Number NNX14AF14G. Part of this work was carried out at the Jet Propulsion Laboratory, California Institute of Technology, under a contract with NASA. PAN data from ARCTAS was provided by Greg Huey supported by NASA Award Number NNX08AR67G. We thank Glenn Diskin for the use of the ARCTAS CO data.

References

Alvarado, M. J., Logan, J. A., Mao, J., Apel, E., Riemer, D., Blake, D., Cohen, R. C., Min, K. E., Perring, A. E., Browne, E. C., Wooldridge, P. J., Diskin, G. S., Sachse, G. W., Fuelberg, H., Sessions, W. R., Harrigan, D. L., Huey, G., Liao, J., Case-Hanks, A., Jimenez, J. L., Cubison, M. J., Vay, S. A., Weinheimer, A. J., Knapp, D. J., Montzka, D. D., Flocke, F. M., Pollack, I. B., Wennberg, P. O.,

Emily Fischer 2/11/2018 5:42 PM
Comment [3]: References were updated in Endnote, and are not automatically highlighted in track changes. These are the new references we added: Pope et al., 2016; Fadnavis et al., 2014; Ungermann et al., 2016; Bowman et al., 2006; Capelle et al., 2014; DeSouza-Machado et al., 2006; Rodgers, 2000; Kluser et al., 2011

Kurten, A., Crounse, J., Clair, J. M. S., Wisthaler, A., Mikoviny, T., Yantosca, R. M., Carouge, C. C., and Le Sager, P.: Nitrogen oxides and PAN in plumes from boreal fires during ARCTAS-B and their impact on ozone: an integrated analysis of aircraft and satellite observations, Atmos. Chem. Phys., 10, 9739-9760, 10.5194/acp-10-9739-2010, 2010.

Alvarado, M. J., Cady-Pereira, K. E., Xiao, Y., Millet, D. B., and Payne, V. H.: Emission Ratios for Ammonia and Formic Acid and Observations of Peroxy Acetyl Nitrate (PAN) and Ethylene in Biomass Burning Smoke as Seen by the Tropospheric Emission Spectrometer (TES), Atmosphere, 2, 10.3390/atmos2040633, 2011.

Alvarado, M. J., Lonsdale, C. R., Yokelson, R. J., Akagi, S. K., Coe, H., Craven, J. S., Fischer, E. V., McMeeking, G. R., Seinfeld, J. H., Soni, T., Taylor, J. W., Weise, D. R., and Wold, C. E.: Investigating the links between ozone and organic aerosol chemistry in a biomass burning plume from a prescribed fire in California chaparral, Atmos. Chem. Phys., 15, 6667-6688, 10.5194/acp-15-6667-2015, 2015.

Bein, K. J., Zhao, Y., Johnston, M. V., and Wexler, A. S.: Interactions between boreal wildfire and urban emissions, J. Geophy. Res., 113, n/a-n/a, 10.1029/2007JD008910, 2008.

Bowman, K. W., Rodgers, C. D., Sund-Kulawik, S., Worden, J. R., Sarkissian, E., Osterman, G., Steck, T., Luo, M., Eldering, A., Shephard, M. W., Worden, H., Clough, S. A., Brown, P. D., Rinsland, C. P., Lampel, M., Gunson, M., and Beer, R.: Tropospheric emission spectrometer: retrieval method and error analysis, IEEE Geosci. Remote Sens., 44, 1297-1307, 2006.

Brey, S. J., and Fischer, E. V.: Smoke in the City: How Often and Where Does Smoke Impact Summertime Ozone in the United States?, Environ. Sci. Tech., 50, 1288-1294, 10.1021/acs.est.5b05218, 2016.

Brey, S. J., Ruminski, M., Atwood, S., and Fischer, E. V.: Connecting smoke plumes to sources using Hazard Mapping System (HMS) smoke and fire location data over North America, submitted to Atmospheric Chemistry and Physics, acp-2017-245, 2017.

Brice, K. A., Bottenheim, J. W., Anlauf, K. G., and Wiebe, H. A.: Long-term measurements of atmospheric peroxyacetylnitrate (PAN) at rural sites in Ontario and Nova Scotia; seasonal variations and long-range transport, Tellus B, 40B, 408-425, 10.1111/j.1600-0889.1988.tb00113.x, 1988.

Briggs, N. L., Jaffe, D. A., Gao, H., Hee, J. R., Baylon, P. M., Zhang, Q., Zhou, S., Collier, S. C., Sampson, P. D., and Cary, R. A.: Particulate Matter, Ozone, and Nitrogen Species in Aged Wildfire Plumes Observed at the Mount Bachelor Observatory, Aerosol Air Qual. Res., 16, 3075-3087, 2016.

Capelle, V., Chédin, A., Siméon, M., Tsamalis, C., Pierangelo, C., Pondrom, M., Crevoisier, C., Crepeau, L., and Scott, N. A.: Evaluation of IASI-derived dust aerosol characteristics over the tropical belt, Atmos. Chem. Phys., 14, 9343-9362`, 10.5194/acp-14-9343-2014, 2014.

DeSouza-Machado, S. G., Strow, L. L., Hannon, S. E., and Motteler, H. E.: Infrared dust spectral signatures from AIRS, Geophys. Res. Lett., 33, 10.1029/2005GL024364, 2006.

Draxler, R. R., and G.D. Hess: An overview of the HYSPLIT_4 modeling system of trajectories, dispersion, and deposition., Aust. Meteor. Mag., 47, 295-308, 1998.

Emmons, L. K., Arnold, S. R., Monks, S. A., Huijnen, V., Tilmes, S., Law, K. S., Thomas, J. L., Raut, J. C., Bouarar, I., Turquety, S., Long, Y., Duncan, B., Steenrod, S., Strode, S., Flemming, J., Mao, J., Langner, J., Thompson, A. M., Tarasick, D., Apel, E. C., Blake, D. R., Cohen, R. C., Dibb, J., Diskin, G. S., Fried, A., Hall, S. R., Huey, L. G., Weinheimer, A. J., Wisthaler, A., Mikoviny, T., Nowak, J., Peischl, J., Roberts, J. M., Ryerson, T., Warneke, C., and Helmig, D.: The POLARCAT Model Intercomparison Project (POLMIP): overview and evaluation with observations, Atmos. Chem. Phys., 15, 6721-6744, 10.5194/acp-15-6721-2015, 2015.

Fadnavis, S., Schultz, M. G., Semeniuk, K., Mahajan, A. S., Pozzoli, L., Sonbawne, S., Ghude, S. D., Kiefer, M., and Eckert, E.: Trends in peroxyacetyl nitrate (PAN) in the upper troposphere and lower stratosphere over southern Asia during the summer monsoon season: regional impacts, Atmos. Chem. Phys., 14, 12725-12743, 10.5194/acp-14-12725-2014, 2014.

Fischer, E. V., Jaffe, D. A., and Weatherhead, E. C.: Free tropospheric peroxyacetyl nitrate (PAN) and ozone at Mount Bachelor: potential causes of variability and timescale for trend detection, Atmos. Chem. Phys., 11, 5641-5654, 10.5194/acp-11-5641-2011, 2011.

Fischer, E. V., Jacob, D. J., Yantosca, R. M., Sulprizio, M. P., Millet, D. B., Mao, J., Paulot, F., Singh, H. B., Roiger, A., Ries, L., Talbot, R. W., Dzepina, K., and Pandey Deolal, S.: Atmospheric peroxyacetyl nitrate (PAN): a global budget and source attribution, Atmos. Chem. Phys., 14, 2679-2698, 10.5194/acp-14-2679-2014, 2014.

Giglio, L., Descloitres, J., Justice, C. O., and Kaufman, Y. J.: An Enhanced Contextual Fire Detection Algorithm for MODIS, Remote Sens. Environ., 87, 273-282, 10.1016/S0034-4257(03)00184-6, 2003.

Giglio, L., Csiszar, I., and Justice, C. O.: Global distribution and seasonality of active fires as observed with the Terra and Aqua Moderate Resolution Imaging Spectroradiometer (MODIS) sensors, J. Geophys. Res., 111, n/a-n/a, 10.1029/2005JG000142, 2006.

Glatthor, N., von Clarmann, T., Fischer, H., Funke, B., Grabowski, U., Höpfner, M., Kellmann, S., Kiefer, M., Linden, A., Milz, M., Steck, T., and Stiller, G. P.: Global peroxyacetyl nitrate (PAN) retrieval in the upper troposphere from limb emission spectra of the Michelson Interferometer for Passive Atmospheric Sounding (MIPAS), Atmos. Chem. Phys., 7, 2775-2787, 10.5194/acp-7-2775-2007, 2007.

Gyawali, M., Arnott, W. P., Lewis, K., and Moosmüller, H.: In situ aerosol optics in Reno, NV, USA during and after the summer 2008 California wildfires and the influence of absorbing and non-absorbing organic coatings on spectral light absorption, Atmos. Chem. Phys., 9, 8007-8015, 10.5194/acp-9-8007-2009, 2009.

Hecobian, A., Liu, Z., Hennigan, C. J., Huey, L. G., Jimenez, J. L., Cubison, M. J., Vay, S., Diskin, G. S., Sachse, G. W., Wisthaler, A., Mikoviny, T., Weinheimer, A. J., Liao, J., Knapp, D. J., Wennberg, P. O., Kürten, A., Crounse, J. D., Clair, J. S., Wang, Y., and Weber, R. J.: Comparison of chemical characteristics of 495 biomass burning plumes intercepted by the NASA DC-8 aircraft during the

ARCTAS/CARB-2008 field campaign, Atmos. Chem. Phys., 11, 13325-13337, 10.5194/acp-11-13325-2011, 2011.

Hurteau, M. D., Westerling, A. L., Wiedinmyer, C., and Bryant, B. P.: Projected Effects of Climate and Development on California Wildfire Emissions through 2100, Environ. Sci. Tech., 48, 2298-2304, 10.1021/es4050133, 2014.

Jaffe, D. A., Wigder, N., Downey, N., Pfister, G., Boynard, A., and Reid, S. B.: Impact of Wildfires on Ozone Exceptional Events in the Western U.S, Environ. Sci. Tech., 47, 11065-11072, 10.1021/es402164f, 2013.

Jiang, Z., Worden, J. R., Payne, V. H., Zhu, L., Fischer, E., Walker, T., and Jones, D. B. A.: Ozone export from East Asia: The role of PAN, J. Geophy. Res., 121, 6555-6563, 10.1002/2016JD024952, 2016.

Kanamitsu, M.: Description of the NMC Global Data Assimilation and Forecast System, Wea. Forecasting, 4, 335-342, 10.1175/1520-0434(1989)004<0335:DOTNGD>2.0.CO;2, 1989.

Kasibhatla, P. S., Levy, H., and Moxim, W. J.: Global NO x , HNO3, PAN, and NO y distributions from fossil fuel combustion emissions: A model study, J. Geophy. Res., 98, 7165-7180, 10.1029/92JD02845, 1993.

Keywood, M., Kanakidou, M., Stohl, A., Dentener, F., Grassi, G., Meyer, C. P., Torseth, K., Edwards, D., Thompson, A. M., Lohmann, U., and Burrows, J.: Fire in the Air: Biomass Burning Impacts in a Changing Climate, Critical Reviews in Environmental Science and Technology, 43, 40-83, 10.1080/10643389.2011.604248, 2013.

Klüser, L., Martynenko, D., and Holzer-Popp, T.: Thermal infrared remote sensing of mineral dust over land and ocean: a spectral SVD based retrieval approach for IASI, Atmos. Meas. Tech., 4, 757-773, 10.5194/amt-4-757-2011, 2011.

Lindaas, J., Farmer, D. K., Pollack, I. B., Abeleira, A., Zaragoza, J., Flocke, F. M., Roscioli, R., Herndon, S., and Fischer, E. V.: The impact of aged wildfire smoke on ozone photochemistry in the Colorado Front Range, Atmos. Chem. Phys. Discuss., in review, doi:10.5194/acp-2017-171, 2017.

Mills, G. P., Sturges, W. T., Salmon, R. A., Bauguitte, S. J. B., Read, K. A., and Bandy, B. J.: Seasonal variation of peroxyacetylnitrate (PAN) in coastal Antarctica measured with a new instrument for the detection of sub-part per trillion mixing ratios of PAN, Atmos. Chem. Phys., 7, 4589-4599, 10.5194/acp-7-4589-2007, 2007.

Monks, P. S., Archibald, A. T., Colette, A., Cooper, O., Coyle, M., Derwent, R., Fowler, D., Granier, C., Law, K. S., Mills, G. E., Stevenson, D. S., Tarasova, O., Thouret, V., von Schneidemesser, E., Sommariva, R., Wild, O., and Williams, M. L.: Tropospheric ozone and its precursors from the urban to the global scale from air quality to short-lived climate forcer, Atmos. Chem. Phys., 15, 8889-8973, 10.5194/acp-15-8889-2015, 2015.

Moore, D. P., and Remedios, J. J.: Seasonality of Peroxyacetyl nitrate (PAN) in the upper troposphere and lower stratosphere using the MIPAS-E instrument, Atmos. Chem. Phys., 10, 6117-6128, 10.5194/acp-10-6117-2010, 2010.

Moritz, M. A., Parisien, M.-A., Batllori, E., Krawchuk, M. A., Van Dorn, J., Ganz, D. J., and Hayhoe, K.: Climate change and disruptions to global fire activity, Ecosphere, 3, 10.1890/ES11-00345.1, 2012.

Morris, G. A., Hersey, S., Thompson, A. M., Pawson, S., Nielsen, J. E., Colarco, P. R., McMillan, W. W., Stohl, A., Turquety, S., Warner, J., Johnson, B. J., Kucsera, T. L., Larko, D. E., Oltmans, S. J., and Witte, J. C.: Alaskan and Canadian forest fires exacerbate ozone pollution over Houston, Texas, on 19 and 20 July 2004, J. Geophy. Res., 111, n/a-n/a, 10.1029/2006JD007090, 2006.

Moxim, W. J., Levy, H., and Kasibhatla, P. S.: Simulated global tropospheric PAN: Its transport and impact on NO x, J. Geophy. Res., 101, 12621-12638, 10.1029/96JD00338, 1996.

Müller, M., Anderson, B. E., Beyersdorf, A. J., Crawford, J. H., Diskin, G. S., Eichler, P., Fried, A., Keutsch, F. N., Mikoviny, T., Thornhill, K. L., Walega, J. G., Weinheimer, A. J., Yang, M., Yokelson, R. J., and Wisthaler, A.: In situ measurements and modeling of reactive trace gases in a small biomass burning plume, Atmos. Chem. Phys., 16, 3813-3824, 10.5194/acp-16-3813-2016, 2016.

Pandey Deolal, S., Henne, S., Ries, L., Gilge, S., Weers, U., Steinbacher, M., Staehelin, J., and Peter, T.: Analysis of elevated springtime levels of Peroxyacetyl nitrate (PAN) at the high Alpine research sites Jungfraujoch and Zugspitze, Atmos. Chem. Phys., 14, 12553-12571, 10.5194/acp-14-12553-2014, 2014.

Parrish, D. D., Trainer, M., Buhr, M. P., Watkins, B. A., and Fehsenfeld, F. C.: Carbon monoxide concentrations and their relation to concentrations of total reactive oxidized nitrogen at two rural U.S. sites, J. Geophy. Res., 96, 9309-9320, 10.1029/91JD00047, 1991.

Payne, V. H., Alvarado, M. J., Cady-Pereira, K. E., Worden, J. R., Kulawik, S. S., and Fischer, E. V.: Satellite observations of peroxyacetyl nitrate from the Aura Tropospheric Emission Spectrometer, Atmos. Meas. Tech., 7, 3737-3749, 10.5194/amt-7-3737-2014, 2014.

Payne, V. H., Fischer, E. V., Worden, J. R., Jiang, Z., Zhu, L., Kurosu, T. P., and Kulawik, S. S.: Spatial variability in tropospheric peroxyacetyl nitrate in the tropics from infrared satellite observations in 2005 and 2006, Atmos. Chem. Phys. Discuss., 2016, 1-21, 10.5194/acp-2016-1047, 2016.

Pfister, G. G., Wiedinmyer, C., and Emmons, L. K.: Impacts of the fall 2007 California wildfires on surface ozone: Integrating local observations with global model simulations, Geophys. Res. Lett., 35, n/a-n/a, 10.1029/2008GL034747, 2008.

Pinder, R. W., Gilliland, A. B., and Dennis, R. L.: Environmental impact of atmospheric NH3 emissions under present and future conditions in the eastern United States, Geophys. Res. Lett., 35, n/a-n/a, 10.1029/2008GL033732, 2008.

Pope, R. J., Richards, N. A. D., Chipperfield, M. P., Moore, D. P., Monks, S. A., Arnold, S. R., Glatthor, N., Kiefer, M., Breider, T. J., Harrison, J. J., Remedios, J. J., Warneke, C., Roberts, J. M., Diskin,

G. S., Huey, L. G., Wisthaler, A., Apel, E. C., Bernath, P. F., and Feng, W.: Intercomparison and evaluation of satellite peroxyacetyl nitrate observations in the upper troposphere–lower stratosphere, Atmos. Chem. Phys., 16, 13541-13559, 10.5194/acp-16-13541-2016, 2016.

Rodgers, C. D.: Inverse methods for atmospheric sounding: the theory and practice, World Sci., Hackensack, N. J., 2000.

Rolph, G. D., Draxler, R. R., Stein, A. F., Taylor, A., Ruminski, M. G., Kondragunta, S., Zeng, J., Huang, H.-C., Manikin, G., McQueen, J. T., and Davidson, P. M.: Description and Verification of the NOAA Smoke Forecasting System: The 2007 Fire Season, Wea. Forecasting, 24, 361-378, 10.1175/2008WAF2222165.1, 2009.

Ruminski, M., Kondragunta, S., Draxler, R. R., and Zheng, W.: Recent changes to the Hazard mapping System, 15th International Emission Inventory Conference: Reinventing Inventories, New Ideas in New Orleans, New Orleans, LA, 2006,

Scholze, M., Knorr, W., Arnell, N. W., and Prentice, I. C.: A climate-change risk analysis for world ecosystems, PNAS, 103, 13116-13120, 2006.

Singh, H. B., and Hanst, P. L.: Peroxyacetyl nitrate (PAN) in the unpolluted atmosphere: An important reservoir for nitrogen oxides, Geophys. Res. Lett., 8, 941-944, 10.1029/GL008i008p00941, 1981.

Singh, H. B.: Reactive nitrogen in the troposphere, Environ. Sci. Tech., 21, 320-327, 10.1021/es00158a001, 1987.

Singh, H. B., Anderson, B. E., Brune, W. H., Cai, C., Cohen, R. C., Crawford, J. H., Cubison, M. J., Czech, E. P., Emmons, L., Fuelberg, H. E., Huey, G., Jacob, D. J., Jimenez, J. L., Kaduwela, A., Kondo, Y., Mao, J., Olson, J. R., Sachse, G. W., Vay, S. A., Weinheimer, A., Wennberg, P. O., and Wisthaler, A.: Pollution influences on atmospheric composition and chemistry at high northern latitudes: Boreal and California forest fire emissions, Atmos. Environ., 44, 4553-4564, 10.1016/j.atmosenv.2010.08.026, 2010.

Singh, H. B., Cai, C., Kaduwela, A., Weinheimer, A., and Wisthaler, A.: Interactions of fire emissions and urban pollution over California: Ozone formation and air quality simulations, Atmos. Environ., 56, 45-51, 10.1016/j.atmosenv.2012.03.046, 2012.

Stein, A. F., Draxler, R. R., Rolph, G. D., Stunder, B. J. B., Cohen, M. D., and Ngan, F.: NOAA's HYSPLIT Atmospheric Transport and Dispersion Modeling System, B. Am. Meteorol. Soc., 96, 2059-2077, 10.1175/BAMS-D-14-00110.1, 2015.

Tanimoto, H., Furutani, H., Kato, S., Matsumoto, J., Makide, Y., and Akimoto, H.: Seasonal cycles of ozone and oxidized nitrogen species in northeast Asia 1. Impact of regional climatology and photochemistry observed during RISOTTO 1999–2000, J. Geophy. Res., 107, ACH 6-1-ACH 6-20, 10.1029/2001JD001496, 2002.

Ungermann, J., Ern, M., Kaufmann, M., Müller, R., Spang, R., Ploeger, F., Vogel, B., and Riese, M.: Observations of PAN and its confinement in the Asian summer monsoon anticyclone in high spatial resolution, Atmos. Chem. Phys., 16, 8389-8403, 10.5194/acp-16-8389-2016, 2016.

Val Martin, M., Heald, C. L., Lamarque, J. F., Tilmes, S., Emmons, L. K., and Schichtel, B. A.: How emissions, climate, and land use change will impact mid-century air quality over the United States: a focus on effects at national parks, Atmos. Chem. Phys., 15, 2805-2823, 10.5194/acp-15-2805-2015, 2015.

Wang, Y., Jacob, D. J., and Logan, J. A.: Global simulation of tropospheric O3-NO x -hydrocarbon chemistry: 3. Origin of tropospheric ozone and effects of nonmethane hydrocarbons, J. Geophy. Res., 103, 10757-10767, 10.1029/98JD00156, 1998.

Westerling, A. L., Hidalgo, H. G., Cayan, D. R., and Swetnam, T. W.: Warming and Earlier Spring Increase Western U.S. Forest Wildfire Activity, Science, 313, 940-943, 2006.

Westerling, A. L.: Increasing western US forest wildfire activity: sensitivity to changes in the timing of spring, Philos. Trans. R. Soc. B, 371, 2016.

Wiegele, A., Glatthor, N., Höpfner, M., Grabowski, U., Kellmann, S., Linden, A., Stiller, G., and von Clarmann, T.: Global distributions of C2H6, C2H2, HCN, and PAN retrieved from MIPAS reduced spectral resolution measurements, Atmos. Meas. Tech., 5, 723-734, 10.5194/amt-5-723-2012, 2012.

Wotawa, G., Novelli, P. C., Trainer, M., and Granier, C.: Inter-annual variability of summertime CO concentrations in the Northern Hemisphere explained by boreal forest fires in North America and Russia, Geophys. Res. Lett., 28, 4575-4578, 10.1029/2001GL013686, 2001.

Yokelson, R. J., Andreae, M. O., and Akagi, S. K.: Pitfalls with the use of enhancement ratios or normalized excess mixing ratios measured in plumes to characterize pollution sources and aging, Atmos. Meas. Tech., 6, 2155-2158, 10.5194/amt-6-2155-2013, 2013.

Yue, X., Mickley, L. J., Logan, J. A., and Kaplan, J. O.: Ensemble projections of wildfire activity and carbonaceous aerosol concentrations over the western United States in the mid-21st century, Atmos. Environ., 77, 767-780, 10.1016/j.atmosenv.2013.06.003, 2013.

Zheng, W., Flocke, F. M., Tyndall, G. S., Swanson, A., Orlando, J. J., Roberts, J. M., Huey, L. G., and Tanner, D. J.: Characterization of a thermal decomposition chemical ionization mass spectrometer for the measurement of peroxy acyl nitrates (PANs) in the atmosphere, Atmos. Chem. Phys., 11, 6529-6547, 10.5194/acp-11-6529-2011, 2011.

Zhu, L., Fischer, E. V., Payne, V. H., Worden, J. R., and Jiang, Z.: TES observations of the interannual variability of PAN over Northern Eurasia and the relationship to springtime fires, Geophys. Res. Lett., 42, 7230-7237, 10.1002/2015GL065328, 2015.

Zhu, L., Fischer, E. V., Payne, V. H., Walker, T., Worden, J. R., Jiang, Z., and Kulawik, S. S.: PAN in the Eastern Pacific Free Troposphere: A Satellite View of the Sources, Seasonality, Interannual Variability and Timeline for Trend Detection, J. Geophy. Res., 122, 10.1002/2016JD025868, 2017.

Figures

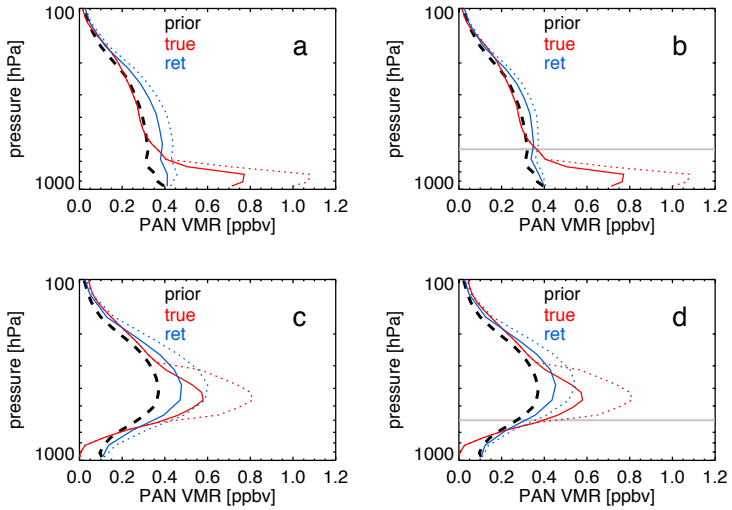

Figure 1: Simulated TES PAN retrievals for four different hypothetical conditions where the black dashed line shows the prior, the two red lines show two different true profiles, and the two blue lines show the retrieved profiles. The true profile exhibits a maximum in the vmr close to the surface in the upper panels (a and b), while the true profile peaks in the mid-troposphere in the lower panels (c and d). Panels on the left (a and c) show clear-sky retrievals while panels on the right (b and d) show retrievals where a cloud with effective optical depth of 0.7 is placed at 600 hPa (dotted line). Corresponding averaging kernels are provided in the Supplementary Information.

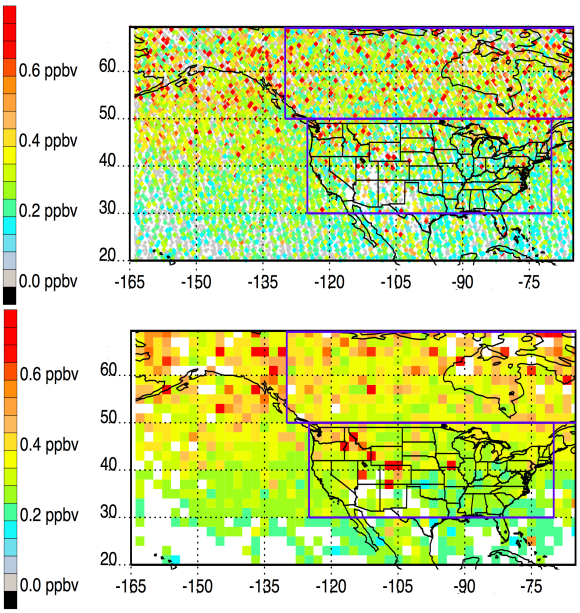

Unknown
Formatted: Font:(Default) Times New Roman, 10 pt

770 **Figure 2**: Average tropospheric PAN in retrievals (DOF > 0.6) during July 2006 – July 2009 (top), and those retrievals averaged in a 2°x2° grid (bottom). The white areas designate locations with less than 5 measurements during this period. The blue lines surround the regions included in the calculations in Figures 4 and 5: 125° W - 70° W, 30° N – 50° N and 130° W - 65° W, 50° N – 70° N.

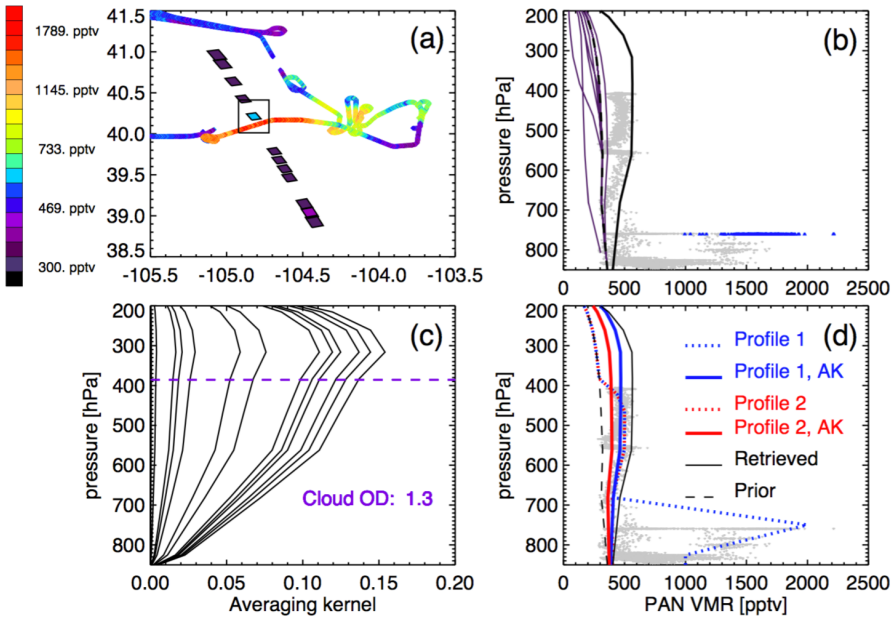

Figure 3: a) Map showing FRAPPÉ aircraft and TES tropospheric average satellite observations of PAN over the Colorado Front Range on 29 July 2014. We define the tropospheric average for a given retrieval as the average retrieved PAN between 800 hPa and the tropopause. TES data show elevated PAN near the location where the aircraft data show highest values for that day. b) All aircraft observations for 29 July 2014 are shown in grey. Blue points show aircraft data within 0.1° longitude and 0.2° latitude of the most elevated TES PAN observation. TES retrieved PAN profiles for 29 July 2014 are also shown. The elevated case is shown by the solid black line, while other cases are shown in purple solid lines. The black dashed line shows the TES a priori profile used in these retrievals. c) TES averaging kernels for this case. The retrieval indicates that a high cloud is present, with optical depth 1.3, leading to reduced sensitivity below the cloud. d) The blue dotted line shows a profile constructed to approximate the aircraft measurements, where PAN is highly elevated in the lower atmosphere. The blue solid line shows this same profile after smoothing with the TES prior and averaging kernel matrix for this scene. The red dotted line shows a hypothetical profile with no enhancement below 680 hPa, while the red solid line shows that same profile smoothed with the TES prior and averaging kernel.

Emily Fischer 1/19/2018 2:52 PM
Deleted: 2

Emily Fischer 1/19/2018 3:09 PM
Moved up [1]: The difference between the red and the blue solid lines indicates that TES has sensitivity to the boundary layer enhancement in this case.

Emily Fischer 1/19/2018 3:11 PM
Deleted: …he difference between the red red and the blue solid lines indicates that TES has sensitivity to the boundary layer enhancement in this case.

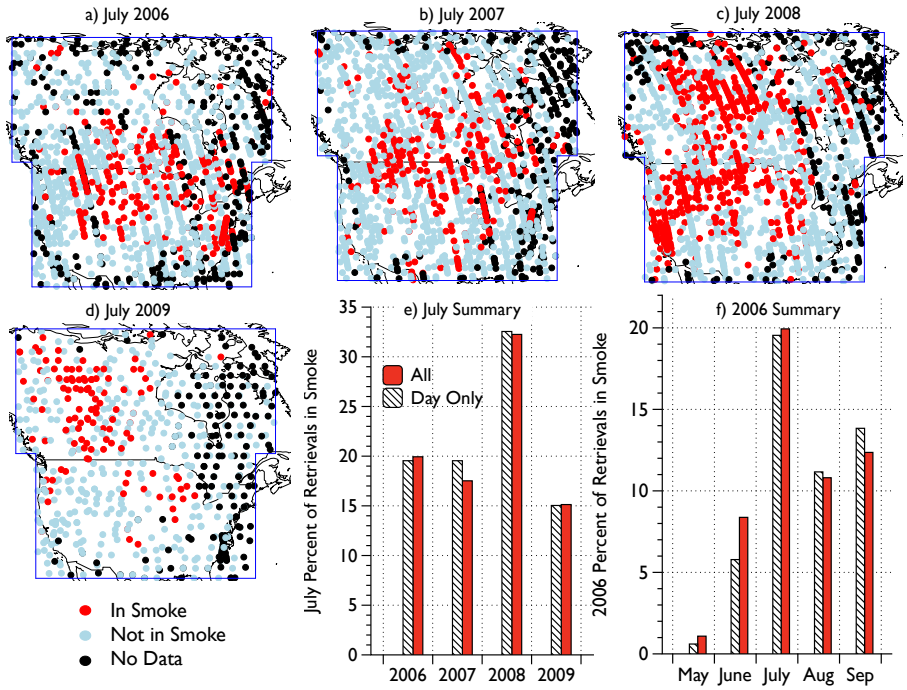

Figure 4: Panels a) through d): PAN TES retrievals with DOF> 0.6 co-located with NOAA Hazard Mapping System smoke polygons (red), and PAN TES retrievals with DOF > 0.6 not co-located with NOAA Hazard Mapping System smoke polygons (grey). The black dots indicate PAN TES retrievals with DOF > 0.6 during times with no NOAA HMS data. The blue lines surround the regions included in the distributions shown in Figure 5: 125° W - 70° W, 30° N – 50° N and 130° W - 65° W, 50° N – 70° N. e) Percent of TES PAN retrievals overlapping HMS smoke plume polygons for July 2006 – 2009. f) Percent of TES PAN retrievals overlapping HMS smoke plume polygons for May – September 2006. In panels e) and f) the red bars indicate the percentage of all retrievals overlapping smoke plumes, and the striped bars indicate the percentage of daytime retrievals overlapping smoke plumes. Pairing was done using the matching UTC day.

Emily Fischer 1/19/2018 2:52 PM
Deleted: 3

Emily Fischer 2/11/2018 5:45 PM
Deleted: calculations in

Emily Fischer 2/7/2018 9:05 AM
Deleted: Figures 2

Emily Fischer 2/7/2018 9:05 AM
Deleted: and 4

Emily Fischer 2/7/2018 9:05 AM
Deleted: 60°

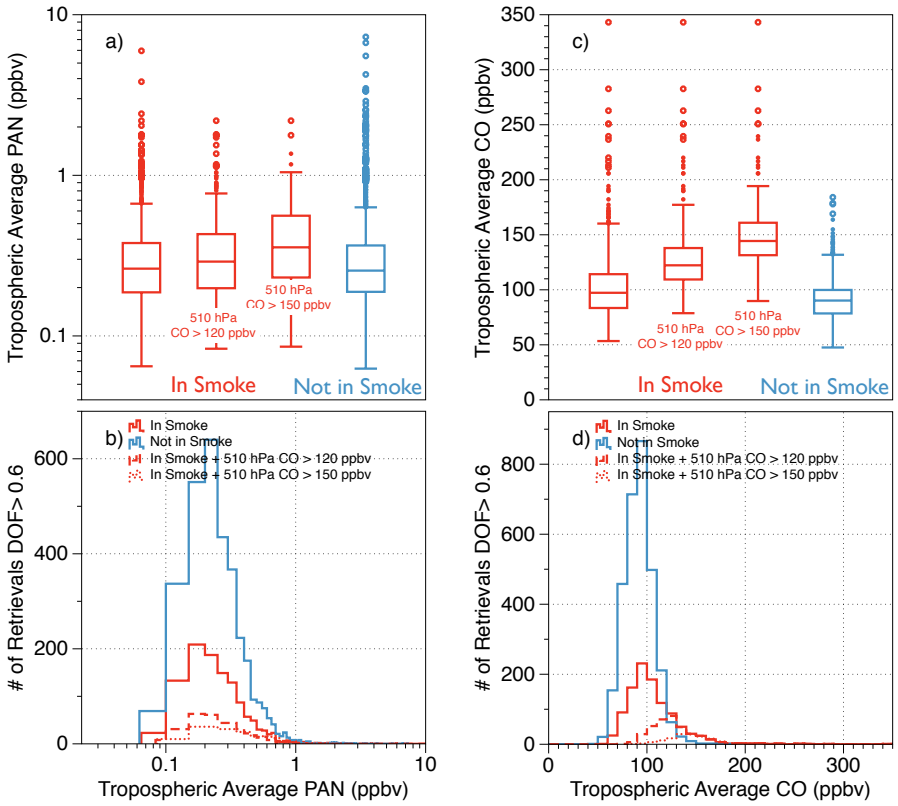

820 **Figure 5:** a) Box plots of July 2006 – 2009 North American TES PAN retrievals overlapping HMS smoke plume polygons ("In Smoke"; red; N =1151), TES PAN retrievals not overlapping HMS smoke plume polygons ("Not In Smoke"; blue-grey; N = 2917), and TES PAN retrievals that overlap HMS smoke plumes and coincide with 510 hPa CO greater than either 120 ppbv (N = 255) or 150 ppbv (N = 139). b) Histograms of July 2006 – 2009 TES PAN retrievals segregated as in a). c) Box plots of July 2006 – 2009
825 TES CO retrievals coincident with the TES PAN retrievals segregated as in a). d) Histograms of July 2006 – 2009 TES CO retrievals coincident with the TES PAN retrievals segregated as in a). The box plots display the interquartile range for each subset and the dots represent outliers.

Emily Fischer 1/19/2018 2:52 PM
Deleted: 4

830

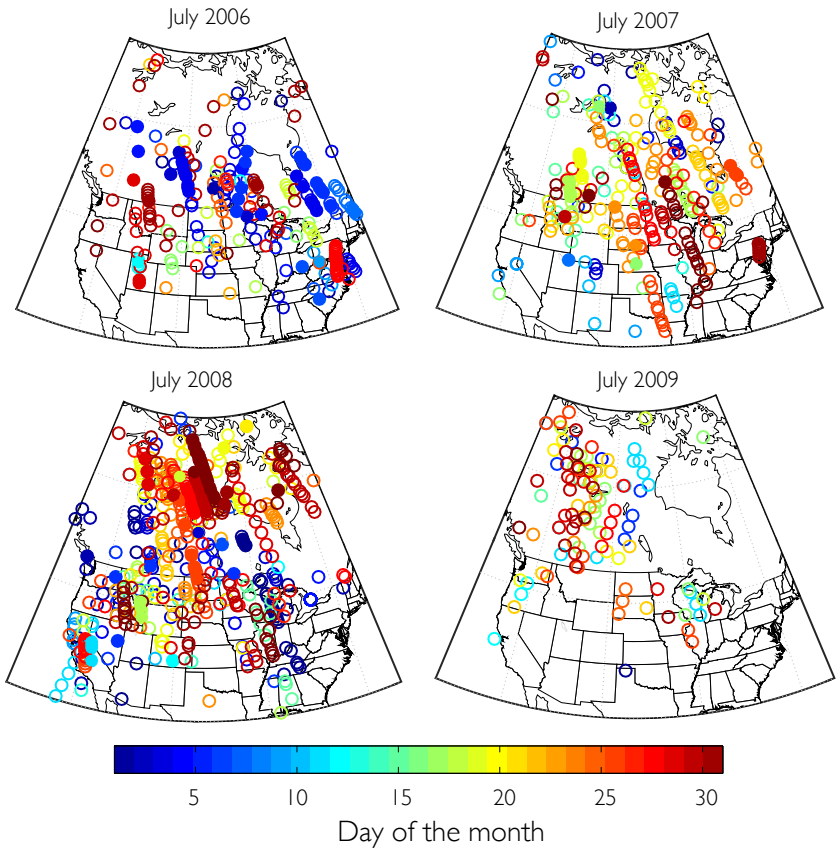

Figure 6: Successful TES PAN retrievals overlapping NOAA HMS smoke polygons for July 2006 to July 2009 colored by the day of the month. Filled circles denote the set of retrievals that also coincide with 510 hPa CO greater than 150 ppbv. This set of point is used to calculated PAN enhancement ratios relative to CO in Figure 8.

Emily Fischer 1/19/2018 2:52 PM
Deleted: 5

Emily Fischer 1/19/2018 2:52 PM
Deleted: 7

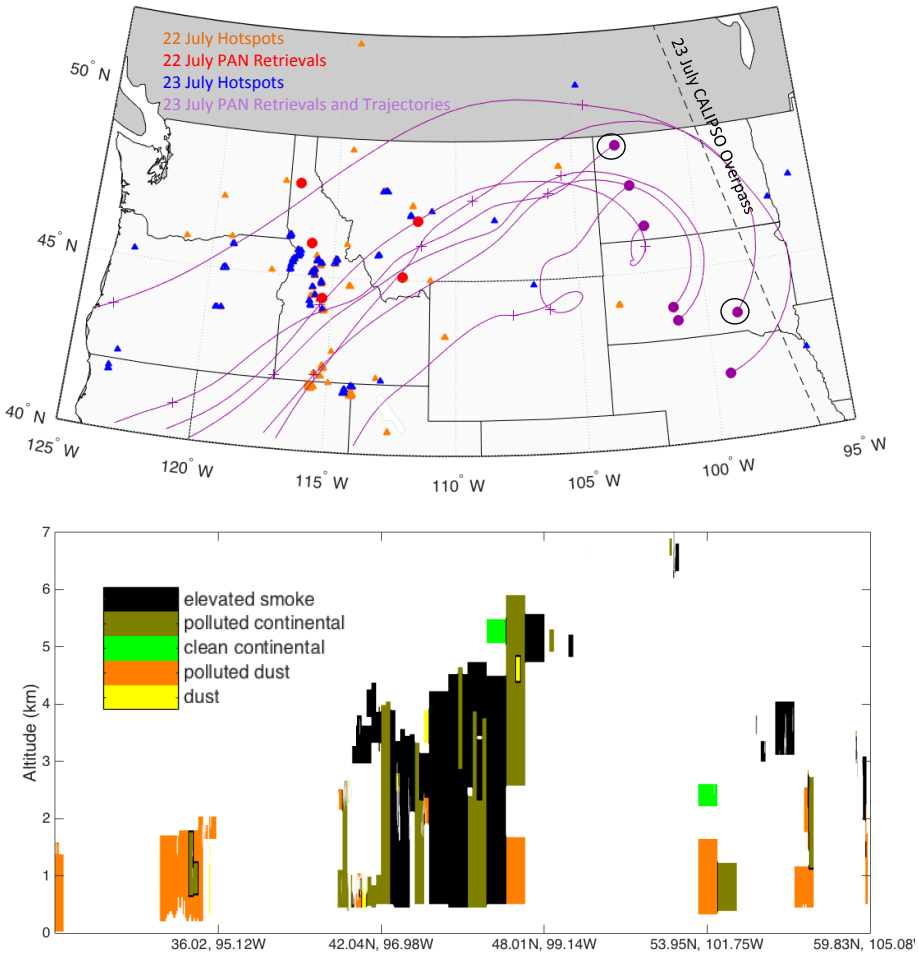

Figure 7: Top panel: Case study of TES PAN retrievals overlapping HMS smoke polygons 22 – 23 July 2007. Orange triangles represent FIRMS MODIS Hotspots for 22 July (Product MCD14ML; https://firms.modaps.eosdis.nasa.gov/download/request.php). Blue triangles represent FIRMS MODIS Hotspots for 23 July. Red circles indicate TES PAN retrievals on 22 July, and purple circles represent TES PAN retrievals on 23 July. We have circled the two retrievals in this set with 510 hPa CO greater than 150 ppbv. The PAN enhancement ratios for these points are noted in Figure 7. The purple '+' signifies 24 hours of transport time on the 4 km trajectories. The black dashed line shows the location of the CALIPSO swath shown in the lower panel. Lower panel: CALIPSO aerosol subtype observed on 23 July 2007. CALIPSO Science Team (2016), CALIPSO/CALIOP Level 2, Vertical Feature Mask Data, version 4.10, Hampton,

Emily Fischer 1/19/2018 2:52 PM
Deleted: 6

VA, USA: NASA Atmospheric Science Data Center (ASDC), Accessed by Emily V. Fischer at doi: 10.5067/CALIOP/CALIPSO/LID_L2_VFM-Standard-V4-10

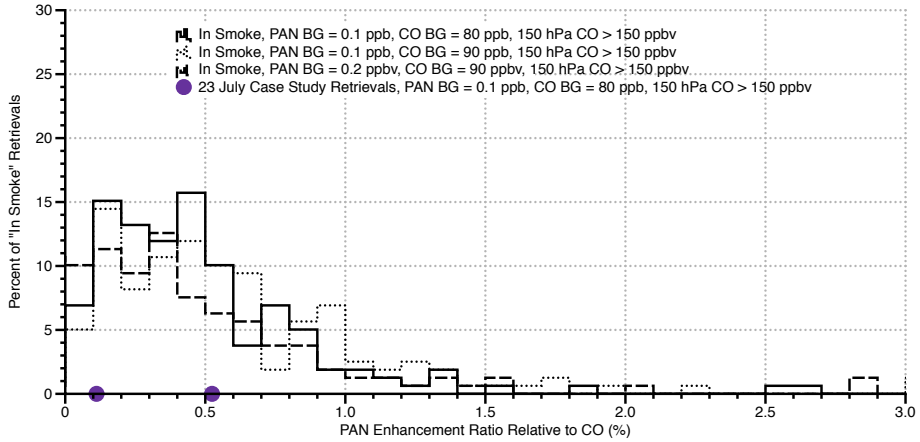

Figure 8: Histogram of estimated PAN enhancement ratios based on tropospheric mean PAN and CO from July 2006 – 2009 North American TES PAN retrievals overlapping HMS smoke plume polygons. The solid black line represents enhancement ratios calculated using an assumed PAN background of 0.1 ppbv with an assumed CO background of 80 ppbv. The dotted black line represents enhancement ratios calculated using an assumed PAN background of 0.1 ppbv with an assumed CO background of 90 ppbv. These specific enhancement ratios were calculated using an assumed CO background of 80 ppbv, similar to the solid black line. The dashed line represents enhancement ratios calculated using a significantly higher assumed PAN background of 0.2 ppbv with an assumed CO background of 90 ppbv. In all cases, negative values are not shown. The purple dots are the enhancement ratios for the two circled retrievals on 23 July 2007 plotted in Figure 7 associated with transported smoke.

Emily Fischer 1/19/2018 2:53 PM
Deleted: 7

Emily Fischer 1/16/2018 3:27 PM
Deleted: red

Emily Fischer 1/16/2018 3:27 PM
Deleted: red

Emily Fischer 1/16/2018 3:29 PM
Deleted: The red dots are the enhancement ratios for the 5 retrievals on 22 July 2007 plotted in Figure 5 associated with fresh smoke. The purple dots are the enhancement ratios for the 6 retrievals on 23 July 2007 plotted in Figure 5 associated with transported smoke.

Emily Fischer 2/13/2018 11:01 AM
Deleted: red

Emily Fischer 1/16/2018 3:31 PM
Deleted: orange

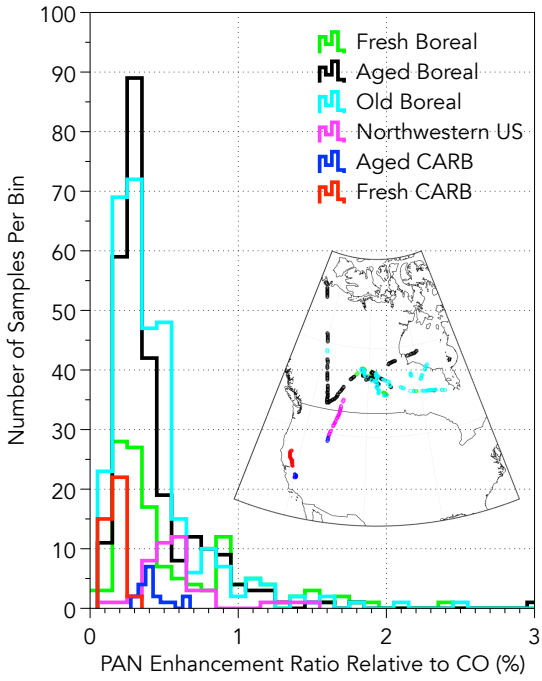

885 **Figure 9:** Histogram of estimated PAN enhancement ratios based on in situ measurements of fire plumes described in Hecobian et al. (2011) from the ARCTAS campaign. Enhancement ratios were calculated using the 25th percentile for each trace gas during the corresponding flight day. These ratios were calculated using the 1-minute merged data.

Emily Fischer 1/19/2018 2:53 PM
Deleted: 8

890